

UNIVERSITY OF OKLAHOMA
GRADUATE COLLEGE

ASSESSMENT OF STRATOSPHERIC WAVE ACTIVITY ASSOCIATED WITH THE
MADDEN-JULIAN OSCILLATION (MJO) AND ITS POTENTIAL IMPACT ON THE
QUASI-BIENNIAL OSCILLATION (QBO)

A THESIS
SUBMITTED TO THE GRADUATE FACULTY
in partial fulfillment of the requirements for the
Degree of
MASTER OF SCIENCE IN METEOROLOGY

By
SADIKSHA RAI
Norman, Oklahoma
2021

ASSESSMENT OF STRATOSPHERIC WAVE ACTIVITY ASSOCIATED WITH THE
MADDEN-JULIAN OSCILLATION (MJO) AND ITS POTENTIAL IMPACT ON THE
QUASI-BIENNIAL OSCILLATION (QBO)

A THESIS APPROVED FOR THE
SCHOOL OF METEOROLOGY

BY THE COMMITTEE CONSISTING OF

Dr. Naoko Sakaeda, Chair

Dr. Jason Furtado

Dr. Cameron Homeyer

Acknowledgments

First and foremost, I would like to thank my advisor, Dr. Naoko Sakaeda, for her teachings, patience, encouragement, endless help (be it with coursework, thesis, or programming), and her immense trust in me, which is why I can stand in this position right now. It would have been a disturbingly rough path for me if not for her help and guidance. I would also like to express thanks to my committee members, Dr. Jason Furtado, and Dr. Cameron Homeyer, for granting me their esteemed time employing suggestions and reviewing my thesis to complete my Masters degree. I want to extend my gratitude towards my family in Nepal without whom I am nothing and to their dedication to raising me to be the independent person I am today. Massive appreciation goes for my husband who is always there for me and helps me to cope in the tiresome pandemic situation and support emotionally for most of my Masters degree journey and continues. I would also like to express my gratitude to my office mates and friends in the School of Meteorology, who supported me throughout this journey. Last but not the least, I would like to express monumental appreciation to the University of Oklahoma for granting the funding, European Center for Medium-Range Weather Forecasts (ECMWF), National Oceanographic and Atmospheric Administration (NOAA), Research Institute for Sustainable Humanosphere (RISH), Kyoto University and National Institute of Aeronautics and Space of Indonesia (LAPAN) for making data accessible to accomplish this research.

Table of Contents

Acknowledgments	iv
Table of Contents	v
List of Figures	vi
Abstract	ix
1. Introduction	1
2. Reassessment of the MJO-QBO Relationship	6
2.1 <i>Outgoing Longwave Radiation based MJO Index (OMI) and Realtime Multivariate MJO Index</i>	6
2.2 <i>ERA-Interim Data</i>	7
2.3 <i>ERA5 Data</i>	7
2.4 <i>Single-level QBO-Index</i>	7
2.4.1 <i>Empirical Orthogonal Function (EOF)-based QBO Index</i>	8
2.5 <i>The MJO Impacts on the QBO Downward Propagation Speed</i>	10
3 The MJO Impacts on Stratospheric Waves Activity in Reanalysis	15
3.1 <i>Intra-seasonal Evolution of the Stratosphere with the MJO</i>	15
3.2 <i>Power Spectrum Analysis</i>	18
3.3 <i>Combined Effects of the QBO and the MJO on Stratospheric Waves</i>	25
4 Re-evaluation of the Stratospheric Waves Activity using Radar Observational Data	29
5 Summary	35
5.1 <i>Review of motivations and methods</i>	35
5.2 <i>Review of Results</i>	35
5.3 <i>Caveats and Recommendations for Future Work</i>	37
REFERENCES	38

List of Figures

Figure 1: Annotated figure from (Son et al., 2017b). The left panel shows observed zonal wind, the middle shows temperature, and the right panel shows vertical temperature gradient anomalies averaged over six Integrated Global Radiosonde Archive (IGRA) stations around the Maritime Continent, during QBOE (blue) and QBOW (red) winters. 4

Figure 2: (a) Vertical structure of the two leading EOFs (EOF1 is represented by blue and EOF2 is represented by dashed green) with the total variance of 81.65 % for normalized monthly mean zonal wind anomalies averaged meridionally from 10°S/N for the vertical extent of 100 hPa to 10 hPa. (b) Different phases of the QBO based on EOF analysis with PC1 as the x-axis and PC2 as the y-axis of the same data as in panel (a). 9

Figure 3: (a) Variation of the MJO activities denoted by normalized OMI amplitude during different phases of the QBO which is statistically significant proved by the bootstrapping method. (b) Vertical profile of the normalized monthly zonal mean zonal wind anomalies depicting the evolution of its easterly and westerly during different phases of the QBO. 10

Figure 4: (a) The relationship of the monthly MJO activities with the monthly downward propagation of the QBO, (i) Under the influence of the QBO itself, represented by red stars and their regression line represented with the solid red line and has a significant correlation coefficient of 0.2, and (ii) After removing the linear dependency of the QBO on its downward propagation, represented by blue crosses and their regression line represented with the dashed blue line. (b) The relationship of the monthly QBO index with the monthly downward propagation of the QBO, denoted by blue stars, and their regression line is represented by the solid blue line and has a significant correlation coefficient of -0.28 . 13

Figure 5: Relationship of the MJO monthly activities with the downward propagation of the QBO during the QBON phase, represented by the stars and corresponding regression line represented by the solid line. The significant correlation coefficient for this relationship is 0.17. 14

Figure 6: Longitude–height cross-section composites of the evolution of stratospheric wave associated during MJO phases 1, 4, 5, and 8 respectively from top to bottom for boreal winter: (a) For Active MJO months, (b) For Inactive MJO months, and (c) For the difference of active and inactive MJO months. Color shading is a 120-days filtered zonal wind anomaly. Shading is the zonal wind anomalies. 16

Figure 7: Longitude height cross-section of composites of the evolution of stratospheric wave for QBON months associated during different MJO phases 1, 4, 5, and 8, respectively from top to bottom for boreal winter: (a) For Active MJO months, (b) For Inactive MJO months and (c) For the difference of active and inactive MJO months. Color shading is a 120-days filtered zonal wind anomaly variance. 18

Figure 8: Climatological power spectrum for ERA-I at 50 hPa with overlaid dispersion curve with an equivalent depth of 300m, 100m, 50m, 25m, and 12m; (a) For symmetric part consisting of Kelvin, Equatorial-Rossby (ER) and Westward Inertia Gravity (WIG)/Eastward Inertia Gravity (EIG) waves denoted by solid, dotted and dashed-and-dotted lines with meridional mode numbers (n) -1, 1 and 1 respectively. Dashed-and-dotted line with n = -1 in the left is for WIG and in the right is for EIG. (b) For antisymmetric part consisting of Mixed Rossby-Gravity (MRG), Eastward Inertia Gravity, and Westward Inertia Gravity Waves denoted by dashed and solid lines. The dashed line with n = 0, in the left, is for MRG and in the right for EIG, on the other hand, a solid line with n = 2, in the left is for WIG, and in the left is for EIG. Shading represents the normalized power of zonal wind anomaly. 20

Figure 9: Same as Figure 8 but for ERA5. 21

Figure 10: Regressed power spectrum for ERA-I at 50 hPa with overlaid dispersion curve with the equivalent depth of 300m, 100m, 50m, 25m, and 12m; (a) For symmetric part consisting of Kelvin, ER, and WIG/Eastward Inertia Gravity (EIG) waves denoted by solid, dotted and dashed-and-dotted lines with meridional mode numbers (n) -1, 1 and 1 respectively. Dashed-and-dotted line with n = -1 in the left is for WIG and in the right is for EIG. (b) For antisymmetric part consisting of MRG, Eastward Inertia Gravity, and WIG-waves denoted by dashed and solid lines. The dashed line with n = 0, in the left, is for MRG and in the right for Eastward Inertia Gravity, on the other hand, a solid line with n = 2, in the left is for WIG, and in the left is for Eastward Inertia Gravity. Shading is the regression coefficient. Contours show the normalized power of zonal wind anomalies. 23

Figure 11: Same as Figure 10, but for ERA5. 24

Figure 12: Same as Figure 10 but for MJO months after removing the QBO related linear signal. 24

Figure 13: Same as Figure 11 but for MJO months after removing the QBO related linear signal. 25

Figure 14: Combined impacts of the MJO and the QBO on stratospheric waves based on ERA-I; (a) For Kelvin Wave, (b) For ER Wave, and (c) For MRG Wave. Shading shows the composites of monthly power of zonal wind anomaly at each QBO and MJO bin for boreal winter. 27

Figure 15: Same as Figure 14 but for ERA5. 28

Figure 16: Climatological power spectrum of zonal wind anomaly for all boreal winter months from 2002-2017; a) For all winter months, and (b) For the difference between QBOE and QBOW months. Shading is the climatological base10 logarithmic values of monthly power of zonal wind anomalies. Green dots represent the region of 95% confidence level in Figure 16b. 30

Figure 17: Power spectrum of zonal wind anomaly regressed on the monthly QBO indices at 50 hPa for boreal winter from 2002-2017. Shading is the values of regression coefficients between

monthly normalized power of zonal wind anomaly and QBO–Index for boreal winter months. Green dots represent the region of 95% confidence level. 31

Figure 18: Power spectrum of zonal wind anomaly after removing QBO signal, regressed on monthly OMI at 50 hPa for boreal winter from 2002 to 2017. Shading is the regression coefficients between monthly normalized power of zonal wind anomaly after removing QBO signal and monthly OMI, for boreal winters only. Green dots represent the region of a 95% confidence level. 32

Figure 19: Composites of normalized monthly power spectrum after removing linear signals associated with the QBO, (a) For active MJO months, (b) For inactive MJO months, and (c) Difference between active and inactive MJO months, during boreal winter only. Green dots elucidates the region of a 95% confidence interval in Figure 19c. 34

Abstract

The Madden-Julian Oscillation (MJO) and Quasi-Biennial Oscillation (QBO) are known to provide sub-seasonal to seasonal predictability, yet their dynamics and interactions are not fully understood. Many recent studies have found that the MJO amplitude tends to be higher during the easterly phase of the QBO while MJO amplitude tends to be weaker during the westerly phase of the QBO over Maritime Continent and warm pool regions during boreal winter. It is often believed that this relationship arises through the modulation of upper-troposphere and lower stratosphere lapse rate by the QBO, but the impacts of the MJO related deep convection on the evolution of the QBO have not been examined in depth.

Vertical momentum fluxes by stratospheric equatorial Kelvin and Rossby-gravity waves generated by tropical deep convection are known to play important roles in the dynamics of the QBO. We hypothesized that the stratospheric waves can be modulated by the MJO convective activities, which can then influence QBO evolution and contribute to the observed MJO-QBO relationship. Therefore, the main objective of this research is to examine potential changes in the stratospheric wave activity associated with the MJO and its potential impacts on the QBO. Our results so far show that enhanced MJO activity is associated with slightly faster downward propagation of the QBO, supporting our hypothesis. However, wavenumber-frequency spectral analysis of ERA-I and ERA5 do not show any MJO impacts on stratospheric wave activity. These contradicting results may be due to the inefficacy of reanalysis to capture high-frequency stratospheric waves or the lack of MJO impacts on stratospheric waves.

To incorporate high-frequency stratospheric waves, we further operate our analysis on radar observational data from the atmospheric Equatorial Atmosphere Radar (EAR) and we notice the presence of higher activities of high-frequency stratospheric waves during an easterly phase of the QBO than a westerly phase of it. We also recognize a subtle but significant linear and non-linear association of high-frequency stratospheric waves with the presence of higher convective activities during active than inactive MJO months. Overall, we couldn't find a strong association of the stratospheric waves (synoptic scale) related to the tropospheric MJO activities, which we hypothesized as the driver of the documented relationship between the MJO and the QBO, hence, implying the MJO as not the modulator of its unique relationship with the QBO.

1. Introduction

The Madden-Julian Oscillation (MJO) is characterized by the planetary-scale convective envelopes that propagate eastward at the speed of around 5 m/s in the equatorial troposphere having an intra-seasonal time scale of about 40–50 days (Madden & Julian, 1971a, 1972a). It is the dominant mode of intra-seasonal variability in the tropical atmosphere and has an extensive influence on global weather and climate (Hendon & Liebmann, 1990; Kessler & Kleeman, 2000). The MJO comprises an eastward progression of large regions of enhanced and suppressed tropical rainfall mainly over the Indian and Pacific basins.

On the other hand, Quasi-Biennial Oscillation (QBO) (Baldwin et al., 2001a) is the dominant mode of interannual variability in the tropical stratosphere with a mean period of about 28 months in which alternating easterly (QBOE), and westerly (QBOW) zonal wind propagate downward with a speed of around 1km/month and is dissipated at the tropical tropopause (Feng, 2019; Son et al., 2017a; Toms et al., 2020). The fundamental dynamics of the QBO are governed by the vertical transport of momentum by equatorial stratospheric waves, triggered by tropical deep convection (Fritts & Alexander, 2003; Geller et al., 1 C.E.; Nishimoto & Yoden, 2017a). The QBO also affects other regions of the atmosphere, including the tropical troposphere, tropical upper stratosphere and mesosphere, and the extratropical middle atmosphere during boreal winter (Baldwin et al., 2001a, 2001b; Baldwin & Dunkerton, 1999; Holton & Austin, 1991; Holton & Tan, 1980, 1982; McIntyre, 1982; Polvani & Kushner, 2002).

Both the MJO and the QBO are well known to have impacts on the Sub-seasonal to Seasonal forecasting (S2S) on a timescale longer than 2 weeks (Baldwin et al., 2001a; Kim et al., 2019; Mundhenk et al., 2018). For example, tropical deep atmospheric convection related to the MJO impacts atmospheric flow in the extratropics resulting in various other impacts enlisted hereafter. The MJO influences the state of the stratospheric polar vortex (Garfinkel et al., 2012, 2014; Kang & Tziperman, 2018a; Liu et al., 2014), Pacific-North American pattern (PNA) (Hsiung Hsu, 1996; Tseng et al., 2019), winter temperature and precipitation variability in southeastern South America (Barrett et al., 2012; Naumann & Vargas, 2010), and winter surface air temperature over Canada and the eastern United States (Lin et al., 2009). The MJO is also well known for modulating atmospheric river activity and associated extreme rainfall in the West Coast region of the U.S (Baggett et al., 2017; Guan et al., 2012; Mundhenk et al., 2017). It is also found that the

MJO influences sudden stratospheric warming events leading to complete reversal of the stratospheric polar vortex, resulting in a negative phase of the Northern Annular Mode (Garfinkel et al., 2014; Garfinkel & Schwartz, 2017; Kang & Tziperman, 2017, 2018a, 2018b). Because of these impacts on global weather and climate, it is essential to understand the underlying dynamics of the initiation of the MJO and its interaction with other atmospheric or oceanic phenomena to improve S2S forecasting.

Likewise, the QBO is also known to impact the weather and climate in different parts of the world. For example, the Northern Hemisphere stratospheric polar vortex is weaker on average in the easterly QBO (QBOE) than in the westerly QBO (QBOW) by 10 ms^{-1} (Anstey & Shepherd, 2014; Holton & Tan, 1980; Pascoe et al., 2005) as the QBO influences the propagation of extratropical large-scale wave activity by modifying the location of zero wind line (Holton & Tan, 1980). Positive Siberian snow anomalies in recent decades are noticed to have concurred with the QBOE years and vice-versa (Douville et al., 2017; Peings et al., 2017). Additionally, during boreal winter, when the QBO is in the easterly phase, the PNA-like Rossby wave teleconnection pattern over the North Pacific is more pronounced than the westerly phase of the QBO (Son et al., 2017b; Toms et al., 2020; J. Wang et al., 2018). Furthermore, it is known that improved ability to simulate stratospheric processes and their impact on surface weather and climate has the potential to improve seasonal and decadal-scale forecasts of surface weather patterns such as North Atlantic Oscillation (NAO) (Marshall & Scaife, 2009; Scaife et al., 2017). All these studies suggest that better understanding the interactions of the QBO with the weather and climate in other parts of the world helps to improve S2S forecasting.

Recent studies found an interesting connection between the MJO and the QBO that the boreal winter MJO activities are enhanced when the QBO zonal wind at 50 hPa is in the easterly phase and are suppressed when the QBO is in the westerly phase (Densmore et al., 2019; Marshall et al., 2017; Nishimoto & Yoden, 2017a; Son et al., 2017b; Zhang & Zhang, 2018). The MJO-QBO relationship is found to be only robust during the boreal winter season (Liu et al., 2014; Sakaeda et al., 2020; Yoo & Son, 2016). More specifically, the QBO appears to influence the MJO, but not the other modes of convection such as convectively coupled equatorial waves (Abhik & Hendon, 2019; Sakaeda et al., 2020), and the relationship appears only after around 1980 (Klotzbach et al., 2019). Besides, when the QBO zonal wind is easterly at 50 hPa, the MJO propagates slowly eastward with a prolonged period of active convection farther into the western

Pacific, however, the MJO convection is largely confined to the west of the Maritime Continent (MC) during the westerly phase of the QBO (Nishimoto & Yoden, 2017a; Son et al., 2017b; S. Wang et al., 2019; Zhang & Zhang, 2018). The reason behind this slower eastward propagation of the MJO during QBO easterlies is possibly due to the stronger convection-circulation coupling associated with the MJO particularly over the MC (Hendon & Abhik, 2018; Son et al., 2017b). It is found that about 40-50% of interannual variability of boreal winter MJO activity is attributed to the QBO (Marshall et al., 2017; Son et al., 2017b), while less than 10% of interannual variability of boreal winter MJO is explained by the El-Nino (Hendon et al., 1999; Hendon & Abhik, 2018; Son et al., 2017b).

To improve the S2S prediction skills, it is essential to capture the MJO-QBO connection with the least error because the MJO prediction skill and its teleconnection patterns are known to be influenced by the QBO (Cassou, 2008; Feng, 2019; Kim et al., 2019; Lin et al., 2009; Martin et al., 2019). However, it is a major challenge to capture the MJO (Ahn et al., 2017, 2020; Hung et al., 2013; Klingaman et al., 2015), and the QBO separately, and their observed relationship in global models (Lee & Klingaman, 2018). For example, S2S models are found to have significant biases in predicting the amplitude and the pattern of the MJO teleconnection. On the other side, simulation of the QBO is a great challenge for general circulation models as they are unable to capture spontaneously generated, realistic QBO. Not only the individual phenomena (i.e., MJO and QBO) but models struggle to capture the MJO-QBO relationship as the simulated MJO-QBO relationship is much weaker than the observed (Back, 2020; Lee & Klingaman, 2018; Martin & Al, 2020), which is associated with weak QBO-induced temperature anomalies in the tropical tropopause or to errors in the MJO vertical structure (Lee & Klingaman, 2018) or biases associated with models in simulating the MJO or the QBO itself (Back, 2020; Martin & Al, 2020). To improve the prediction skills of the MJO, it is essential to simulate individual phenomena and the MJO-QBO connection with the least error.

Even though we know how the changes in the MJO activities are associated with different phases of the QBO, the physical mechanism underlying this relationship is nebulous. The known relationship between the MJO and the QBO is generally considered through the QBO-related changes in the static stability and the vertical zonal wind shear around the tropopause layer (Nishimoto & Yoden, 2017a; Son et al., 2017b; Yoo & Son, 2016). The lower stratosphere has cold temperature anomalies when there are QBO easterlies in the lower stratosphere and vice-

versa, which is in accord with the thermal wind balance (Nishimoto & Yoden, 2017b; Son et al., 2017b). The presence of cold temperature anomalies during QBO easterlies reduces the static stability near the tropopause, destabilizing tropical deep convection observed in recent modeling studies (Martin et al., 2019; Nie & Sobel, 2015) which was hypothesized to promote stronger MJO activity during boreal winter and vice-versa (Hendon & Abhik, 2018; Martin et al., 2019; Nishimoto & Yoden, 2017b; Son et al., 2017b).

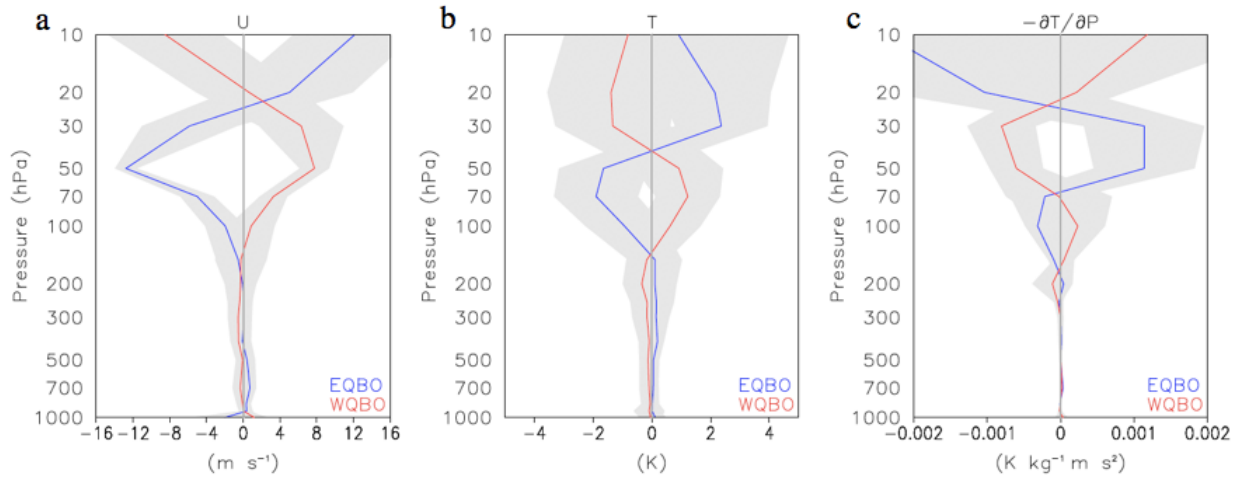


Figure 1: Annotated figure from (Son et al., 2017b). The left panel shows observed zonal wind, the middle shows temperature, and the right panel shows vertical temperature gradient anomalies averaged over six Integrated Global Radiosonde Archive (IGRA) stations around the Maritime Continent, during QBOE (blue) and QBOW (red) winters.

For example, in Figure 1 from Son et al., 2017b where Figures 1a and 1b show the vertical structure of observed zonal wind anomalies and temperature anomalies averaged over six Integrated Global Radiosonde Archive stations around the Maritime Continent, during QBOE (blue) and QBOW (red) winters. There are cold temperature anomalies in the lower stratosphere when QBO there is in its easterly phase and warm temperature anomalies in the lower stratosphere when QBO there is in its westerly phase. Figure 1c shows the vertical structure of the static stability for QBOE and QBOW phases, which shows that there is a reduction in the vertical static stability associated with the cold temperature anomalies around tropopause during the QBOE months and an increase in the vertical static stability associated with the warm temperature anomalies around tropopause during the QBOW months as discussed earlier.

Furthermore, it is also suggested that both warm temperature anomalies in the lower stratosphere and cold temperature anomalies near tropopause at 100 hPa are stronger and robustly related with the MJO convection when QBO is easterly and vice-versa (Hendon & Abhik, 2018).

MJO induced temperature anomalies when acting together with the reduced static stability result in further weakening of the static stability near the tropopause, which ultimately leads to stronger MJO convection during QBOE (Hendon & Abhik, 2018). Many prior studies hypothesize that the MJO-QBO relationship occurs through this one-way impact: the QBO impacts the activities of the MJO while neglecting the possible impacts of the MJO on the QBO dynamics. However, this hypothesized mechanism does not explain why the QBO exclusively influences the MJO, but no other modes of convectively-coupled equatorial waves (Sakaeda et al., 2020). In addition, recent numerical experiments cannot replicate the observed MJO-QBO relationship simply by adding QBO-induced temperature and static stability anomalies in the upper troposphere and lower stratosphere. These results indicate that an alternative hypothesis must be explored to explain the MJO-QBO relationship.

As we know that the MJO is the most prominent intra-seasonal tropical phenomenon associated with deep convection (Madden & Julian, 1971b, 1972b), and the dynamics of the QBO is known to get modulated by the stratospheric equatorial waves such as Kelvin and Rossby-Waves (Baldwin et al., 2001b, 2001a), which are intrinsically generated by the tropical deep convection. Hence, it could be possible that the observed MJO-QBO relationship is the result of the modulation of the stratospheric wave activities associated with the MJO activities. Therefore, we hypothesize that the variability in the MJO convective activities in the troposphere can alter stratospheric waves and associated momentum fluxes, which thus modulates the evolution of the QBO and then, resulting in the observed MJO-QBO relationship. While this is a plausible mechanism, no prior studies have tested this hypothesis. Therefore, this study will address the following questions by combining observational and reanalysis datasets:

- Does the MJO influence stratospheric wave activities?
- If it does, could this be the mechanism driving the documented MJO-QBO relationship?

2. Reassessment of the MJO-QBO Relationship

This chapter will be revisiting the MJO-QBO relationship based on Empirical Orthogonal Function (EOF) analysis so that we can analyze the MJO-QBO relationship in the greater vertical structure of stratospheric zonal winds rather than only 50 hPa which is often used in prior studies. The main motto behind using greater vertical extent is its ability to analyze the descent rate of the QBO from the upper stratosphere until it dissipates at 50 hPa and associated changes in QBO dynamics with tropics generated waves related to the MJO. The analyses of this study focus on the boreal winter i.e., DJF from 1979 to 2017, because the relationship between the MJO and the QBO is significant only during that period of the year.

2.1 *Outgoing Longwave Radiation based MJO Index (OMI) and Realtime Multivariate MJO Index*

To define the amplitude of the MJO and phase of the MJO, we have used outgoing longwave radiation (OLR)–based MJO index (OMI, Kiladis, et al., 2014). The OMI consists of the leading pair of empirical orthogonal functions of bandpass-filtered OLR over 20°S–20°N. It is obtained by projecting 20–96 day filtered OLR anomalies, including all eastward and westward wave numbers, onto the leading EOF patterns of 30–96 days eastward filtered OLR. The resultant two leading principal components, PC1, and PC2 are available from the NOAA Physical Sciences Laboratory website (<https://psl.noaa.gov/mjo/mjoindex/>). OMI is solely based on the satellite-derived OLR and is known to discriminate the convective signal of the MJO more directly.

We use the OMI index to identify months of active and inactive MJO to assess the impacts of MJO activity on the equatorial stratospheric waves and the QBO. OMI amplitude is first averaged monthly. To identify the months of active and inactive MJO, the seasonal cycle is removed from this monthly OMI and then the anomaly is normalized using the monthly standard deviation of each month of the year. After that, we defined the active and inactive months of the MJO based on this normalized monthly OMI amplitude.

We also test the sensitivity of some results by using Real-time Multivariate MJO (RMM) Index (M. C. Wheeler & Hendon, 2004). This index uses empirical orthogonal function (EOF) analysis applied to OLR and 200– and 850–hPa zonal wind anomalies, averaged near equatorially for 15°S to 15°N to determine the first two principal components (RMM1 and RMM2). For this

research, we use the observed RMM index available from the Australian Bureau of Meteorology (BOM, <http://www.bom.gov.au/climate/mjo/>). Just like OMI, RMM amplitude is first averaged monthly, and to identify the months of active and inactive MJO, the seasonal cycle is removed from that monthly RMM, and the anomaly is normalized using the monthly standard deviation of each month of the year. Thereafter, the active and inactive months of the MJO are defined based on the normalized monthly RMM amplitude.

2.2 *ERA-Interim Data*

We will use 6 hourly zonal wind and monthly mean-zonal wind ERA-I reanalysis data from the European Center for Medium-Range Weather Forecasts (ECMWF) having a spatial resolution of $0.7^\circ \times 0.7^\circ$ and vertical resolution from the surface up to 1 hPa of 20 levels (Dee et al., 2011). ERA-Interim's 50 hPa monthly zonal mean zonal wind data is used to diagnose the state of the QBO from 1979 to 2017.

2.3 *ERA5 Data*

We will also use 6 hourly zonal wind ERA5 data from ECMWF having a spatial resolution of ~ 31 km (i.e., $0.25^\circ \times 0.25^\circ$), vertical resolution from surface to 1 Pa with 137 levels and has an hourly temporal resolution (Hersbach et al., 2020) to diagnose the types of stratospheric waves associated with the QBO and the MJO separately from 1979 to 2017.

2.4 *Single-level QBO-Index*

This study uses two types of QBO indices to identify and re-examine the relationship between the QBO and the MJO. The first one is defined by the normalized monthly zonal mean zonal wind at 50 hPa averaged over 10°S – 10°N using ERA-Interim data, which is the same index used in prior studies that have examined the MJO-QBO relationship (Nishimoto & Yoden, 2017b; Son et al., 2017b; Yoo & Son, 2016). We first removed the seasonal cycle from the monthly zonal wind, and the anomaly is then normalized by using the monthly standard deviation of each month of the year. When the QBO-index is smaller than the -0.5 standard deviation, we define the QBO to be in its easterly phase and when the QBO index is greater than 0.5 standard deviations, the

QBO is in its westerly phase. The QBO is known to be in the neutral phase otherwise. To scrutinize the QBO index sensitivity on latitude, instead of averaging over 10°S–10°N, we averaged over 5°S–5°N for the same periods. And we encounter a significantly small number of changes in the number of months during different phases of the QBO proving that the QBO index is not sensitive to the latitude under consideration within the tropics.

While this index is simple to calculate and to be used, this index is based on a single level, which does not capture the vertical structure of the QBO. Therefore, in this section, we also will be using the EOF-based QBO index to capture the vertical structure and evolution of the QBO. The EOF-based QBO index will also allow us to quantify the monthly downward propagation speed of the QBO, which may be influenced by the MJO.

2.4.1 Empirical Orthogonal Function (EOF)-based QBO Index

EOF analysis of normalized monthly zonal mean zonal wind anomalies averaged meridionally from 10°S to 10°N for the vertical extent of 100 hPa to 10 hPa, are used to identify the QBO following the process described in (Densmore et al., 2019). The sum of first and second leading EOFs accounts for 81.65% of the total variance explained with 49.26% and 32.39%, respectively which are shown in Figure 2a. The corresponding monthly principal components, normalized by their standard deviation are represented as PC1 and PC2 respectively, hereafter. These two PC components are then used to define the phase space of the QBO from which the evolution of the QBO can be analyzed.

$$\text{Phase Angle } (\theta) = \text{Arctan}(PC2/PC1) \dots\dots\dots \text{Eq. (1)}$$

The angle calculated from Eq. 1 around the center of the diagram in Figure 2b indicates the state of the QBO. The distance from the center corresponds to the magnitude of the QBO zonal wind and it moves counterclockwise around the phase space with time as the oscillation propagates downward through the stratosphere. The zonal wind profile generated by the QBO is categorized into eight phases based on the angle in the phase space. QBO phases 2 and 3 represent the month with mid-stratospheric easterly wind anomalies, QBO phases 4 and 5 represent the month with lower-stratospheric easterly wind anomalies, QBO phases 6 and 7 represent the month with mid-

stratospheric westerly wind anomalies, and QBO phases 8 and 1 represent the month with lower-stratospheric westerly wind anomalies.

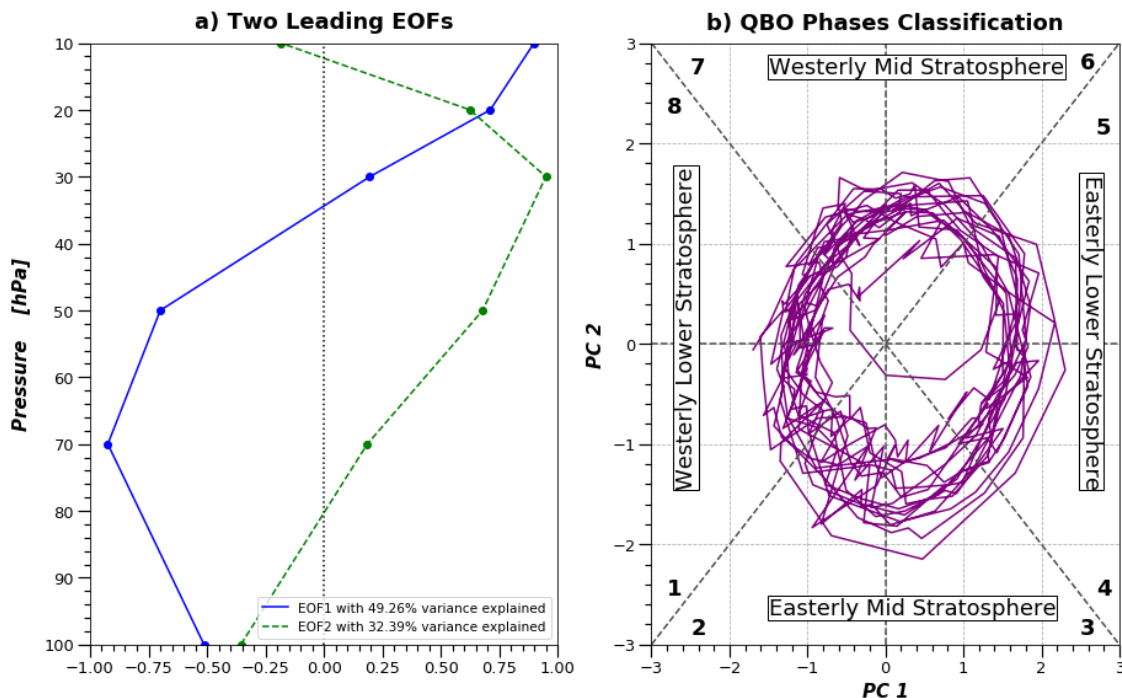


Figure 2: (a) Vertical structure of the two leading EOFs (EOF1 is represented by blue and EOF2 is represented by dashed green) with the total variance of 81.65 % for normalized monthly mean zonal wind anomalies averaged meridionally from 10°S/N for the vertical extent of 100 hPa to 10 hPa. (b) Different phases of the QBO based on EOF analysis with PC1 as the x-axis and PC2 as the y-axis of the same data as in panel (a).

As discussed earlier, the major advantage of using EOF-based analysis to describe the QBO phases is its ability to identify the vertical structure and monthly downward propagation speed of the QBO, which cannot be identified using a single-level, 50 hPa QBO index.

Using the EOF-based QBO index, Figure 3 captures the result associated with the known MJO-QBO relationship where Figure 3a shows the average standardized monthly OMI anomalies during the eight phases of the QBO, and Figure 3b shows the corresponding monthly zonal-mean zonal wind anomalies in the stratosphere. Figure 3 shows that when the QBO in the lower stratosphere is in its easterly phase (i.e., QBO Phases 4-5), there are higher activities of the MJO, which confirm that the result of the EOF analysis is equivalent to the previous studies (Densmore et al., 2019; Marshall et al., 2017; Nishimoto & Yoden, 2017b; Son et al., 2017b; Zhang & Zhang, 2018).

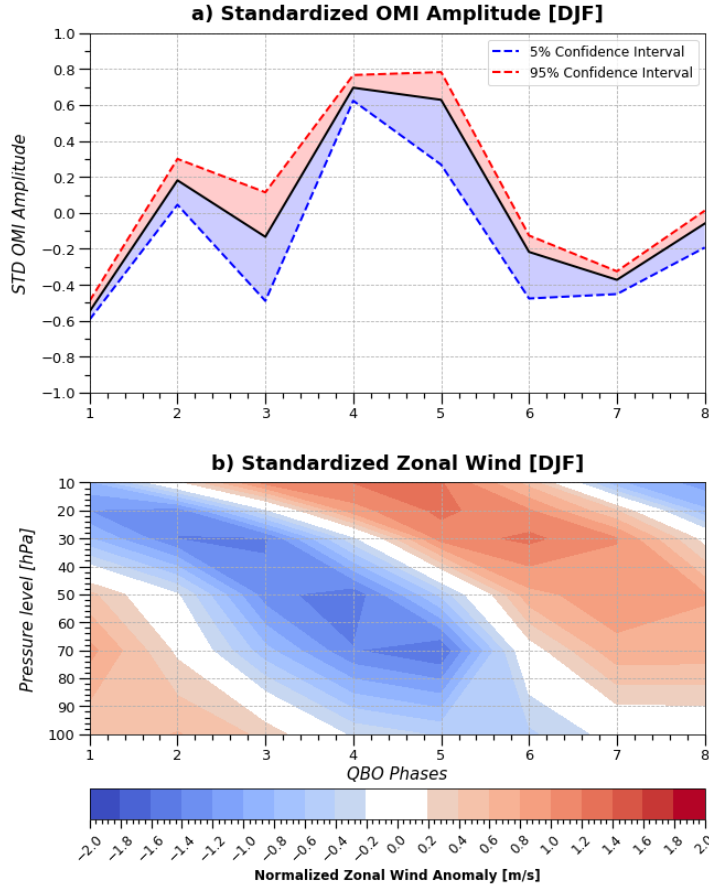


Figure 3: (a) Variation of the MJO activities denoted by normalized OMI amplitude during different phases of the QBO which is statistically significant proved by the bootstrapping method. (b) Vertical profile of the normalized monthly zonal mean zonal wind anomalies depicting the evolution of its easterly and westerly during different phases of the QBO.

2.5 The MJO Impacts on the QBO Downward Propagation Speed

If the MJO modulates the stratospheric wave activity, which influences the downward propagation of the QBO, we expect some relationship between the downward propagation speed of the QBO and MJO monthly activity. We hypothesize faster downward propagation speed of the QBO during active MJO months assuming active MJO convections generate more stratospheric waves and vice-versa. Hence, to do so, we investigate the changes in the downward propagation speed of the QBO related to the MJO activities. The downward propagation of the QBO is estimated by the time rate of change in the QBO phase angle (Eq. 2):

$$\text{Downward Propagation per Month } (\Delta\theta/\text{month}) = \{\theta(t+\Delta t) - \theta(t-\Delta t)\} / (2 \times \Delta t) \dots \dots \dots \text{Eq. (2)}$$

Where $\Delta\theta$ = Change in phase angle,

Δt = change in the number of months

The impact of the MJO convective activity on the QBO downward propagation speed is examined in Figure 4 during DJF. The red stars and corresponding red lines in Figure 4a are the relationship of monthly MJO activities with the monthly downward propagation speed of the QBO and the regression slope between them, respectively. The statistical significance of the regression analysis between normalized OMI and monthly downward propagation speed of the QBO is performed using 1000 iterations of a Monte–Carlo resampling test with repetitions at the 95% confidence level.

The positive slope in Figure 4a indicates that the QBO downward propagation is slightly faster during the months of active MJO. However, it is also known that the QBO westerlies tend to propagate downward faster (Baldwin et al., 2001). Therefore, the downward propagation speed of the QBO must appear faster when QBO easterlies appear in the lower stratosphere (QBO phases 4 and 5), which is when the MJO convective activity also tends to be more active. And as expected, Figure 4b shows that during the QBOW phase, the monthly downward propagation speed of the QBO is slower as compared to the QBOE phase at the lower stratosphere.

Figure 4b also suggests that the relationship between monthly MJO activities and monthly downward propagation of the QBO in the red line of Figure 4a might be partially due to the influence of the QBO on its downward propagation. To eliminate the QBO impacts on the relationship between the monthly MJO activities and the downward propagation speed of the QBO, the linear relationship between the QBO and its monthly downward propagation speed that is reconstructed from a regression model shown in Figure 4b, is removed from the time series of the monthly QBO downward propagation. After that, the QBO bias-free monthly downward propagation speed of the QBO and the monthly MJO activities is examined, and their relationship obtained is shown by the blue cross and lines in Figure 4a. While the regression slope becomes flatter, there is still a positive relationship between monthly MJO convective activity and the QBO downward propagation, suggesting that active MJO convection leads to a small increase in the QBO downward propagation speed. The statistical significance of the result we got for the relationship between the monthly MJO convective activity and the QBO bias-free downward propagation speed of the QBO is performed using 1000 iterations of a Monte-Carlo resampling test with repetitions at the 95% confidence level.

To further test the robustness of the result shown in Figure. 4a, the relationship between the monthly downward propagation speed of the QBO with the monthly MJO activities was also examined during the QBON phase when there is no impact of the QBO. And for that, we found a small but significant positive relationship as shown in black asterisks and black lines in Figure 5. This result advocates faster monthly downward propagation speed of the QBO during higher activities of the MJO and vice-versa even when QBO itself is in its neutral phase and supports the hypothesis for this part of the analysis.

In summary, we find there is a faster monthly downward propagation speed of the QBO corresponding to the higher monthly MJO convective activities and vice-versa. And this result is true either when we linearly remove the QBO impacts on the monthly downward propagation speed of the QBO or when we account for QBON phase periods, supporting our hypothesis that the MJO may impact the QBO by modulating stratospheric wave activity. However, when we repeat the same analysis using RMM Index (M. C. Wheeler & Hendon, 2004), it does not show any significant relationship between monthly MJO activities (indicated by the RMM) and the monthly downward propagation speed of the QBO. This result we get for monthly RMM indices (not shown) unlike OMI, might be since RMM indices are more susceptible to get influenced by other convectively coupled modes in the tropical troposphere else than the MJO that contributed to the loss of actual signal solely related to the MJO activities (Roundy et al., 2009; Straub, 2013).

Although these results from OMI suggest that MJO convective activity impacts the QBO, this finding is not sufficient to claim the impacts of the monthly MJO activities on stratospheric waves as it is hard to detect the actual types of stratospheric waves related to the MJO impacting the dynamics of the QBO. The results also show that the downward propagation speed of the QBO depends exclusively on the type of MJO indices being used to define its period, proving the sensitivity of the MJO-QBO relationship on the type of index used. Thus, the next chapter will further investigate if and how much the MJO impacts stratospheric wave activities that may lead to changes in the QBO downward propagation speed.

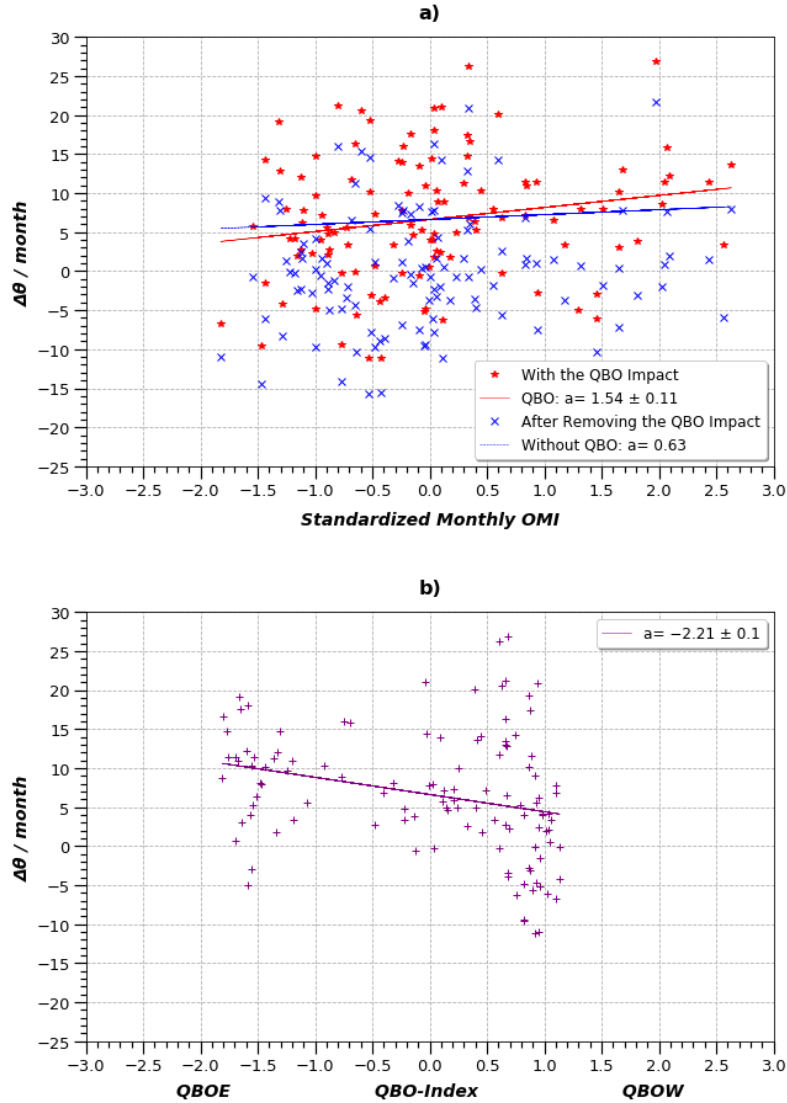


Figure 4: (a) The relationship of the monthly MJO activities with the monthly downward propagation of the QBO, (i) Under the influence of the QBO itself, represented by red stars and their regression line represented with the solid red line and has a significant correlation coefficient of 0.2, and (ii) After removing the linear dependency of the QBO on its downward propagation, represented by blue crosses and their regression line represented with the dashed blue line. (b) The relationship of the monthly QBO index with the monthly downward propagation of the QBO, denoted by blue stars, and their regression line is represented by the solid blue line and has a significant correlation coefficient of -0.28 .

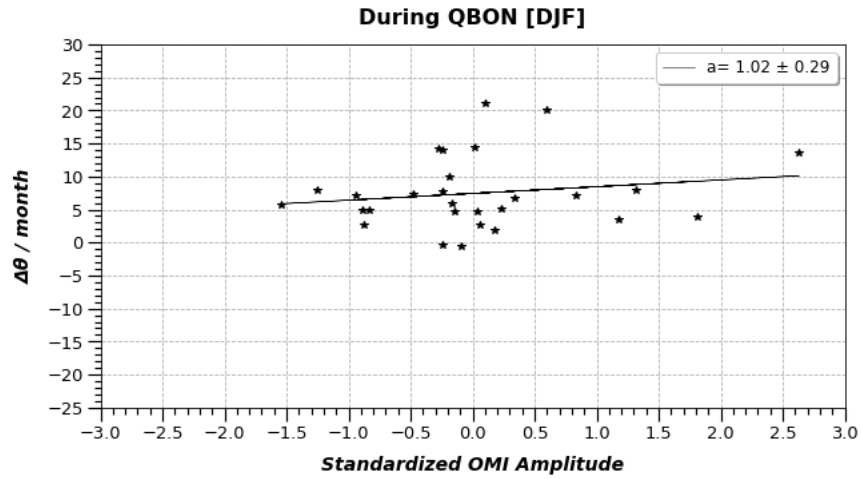


Figure 5: Relationship of the MJO monthly activities with the downward propagation of the QBO during the QBON phase, represented by the stars and corresponding regression line represented by the solid line. The significant correlation coefficient for this relationship is 0.17.

3 The MJO Impacts on Stratospheric Waves Activity in Reanalysis

Since the previous chapter indicated a potential influence of the MJO activities on the monthly downward propagation speed of the QBO, in this chapter we aim to further analyze the possibility of MJO influences on the stratospheric wave activities. To do so, we will examine the intra-seasonal evolution of the stratospheric signals associated with the MJO. Afterward, we will use power spectral analysis to diagnose changes in stratospheric wave activity associated with the MJO and QBO.

3.1 *Intra-seasonal Evolution of the Stratosphere with the MJO*

To comprehend how the MJO may influence the stratosphere, we will first examine the evolution of intra-seasonal stratospheric wind and the variance of higher frequency wind associated with the MJO. Knowing that many prior studies have extensively examined the evolution of tropospheric circulation associated with the MJO, our analysis here will focus on the vertical extent from 200 hPa to 10 hPa and for OMI Phases 1, 4, 5, and 8. The selection of the phases of the MJO is based on the enhanced and suppressed phases of it over MC i.e, in Phase 1 and 8, MJO is in its suppressed phase over MC and in Phases 4 and 5, it is in its enhanced phase over MC.

To do so, we first categorize the MJO into its active and inactive months with the method discussed in section 2.2. From ERA-I 6-hourly zonal wind data, we remove the time-mean and the first three harmonics of the seasonal cycle to generate anomalies. Meanwhile, to eliminate the QBO signal and examine how the intra-seasonal signal differs during active and inactive MJO months, we further remove a 120-days running mean to eliminate the low-frequency signals associated with the QBO. The 6-hourly zonal wind anomalies after removing the QBO signal, are then composited based on the eight OMI phases, separately during the active and inactive MJO months.

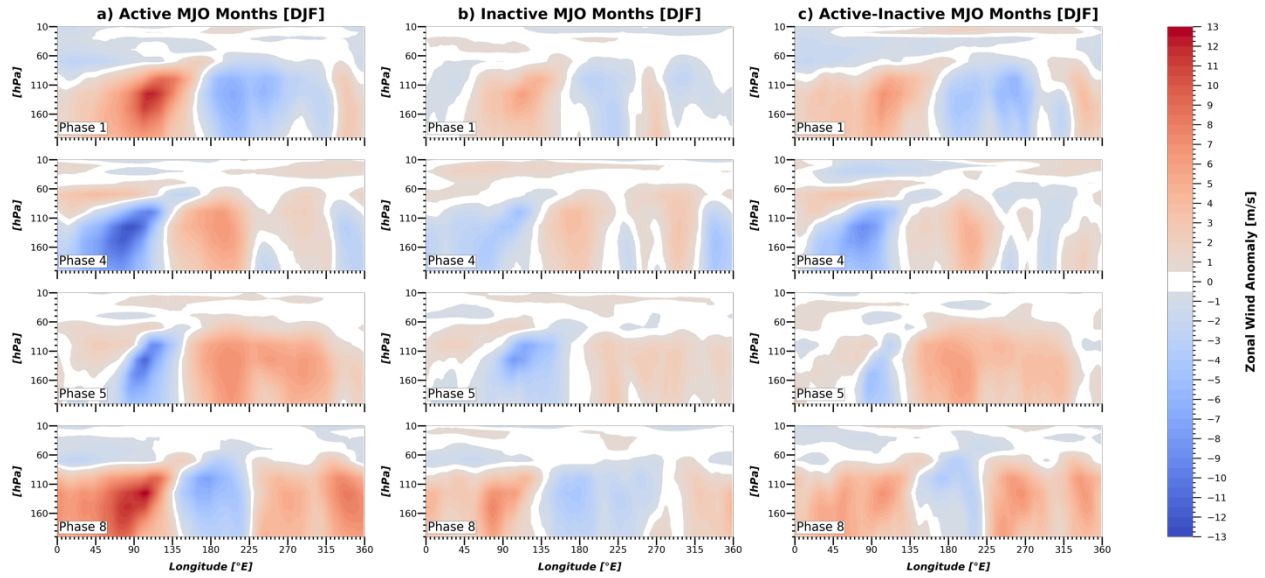


Figure 6: Longitude–height cross-section composites of the evolution of stratospheric wave associated during MJO phases 1, 4, 5, and 8 respectively from top to bottom for boreal winter: (a) For Active MJO months, (b) For Inactive MJO months, and (c) For the difference of active and inactive MJO months. Color shading is a 120-days filtered zonal wind anomaly. Shading is the zonal wind anomalies.

In Figure 6, positive shading (red) represents the presence of westerly wind anomalies and negative shading (blue) represents easterly wind anomalies in intra-seasonal time scales. In Figure 6c (OMI Phase 1 during MJO active months), at around 50 hPa, there is the presence of easterly wind anomalies throughout the entire longitudes, however, during OMI Phase 4, there seems to be the formation of westerly zonal wind anomalies at and below 60 hPa associated with Kelvin like structure with positive tilt shown by blue shading. In OMI Phases 5 and 6 during MJO active months, the zonal wind anomaly is westerly at and above 50 hPa and easterly above 50 hPa to 10 hPa but there seems presence of no wind anomalies at 50 hPa respectively. Overall, this shows when the MJO is in its active months and moves from its one phase to another, the Kelvin wave-like structure formed in the upper troposphere due to the convection related to the MJO in the lower troposphere, influences the intra-seasonal variability of zonal wind anomalies in the lower to upper stratosphere which appears weaker during inactive MJO months as seen in Figure 6b. This result suggests that the MJO influences the stratospheric wave activity at intra-seasonal time scales, however, this result alone is not sufficient to support the strong influence of MJO activities on the variability of the stratospheric waves in interannual time scale.

The zonal wind variability signal shown in Figure 6 is intra-seasonal circulation that does not necessarily indicate how higher-frequency stratospheric wave activity (e.g., Kelvin, and

Rossby-waves) might be influenced by the MJO. Before analyzing the MJO influences in higher-frequency stratospheric wave activity, we want to check if the result we get in Figure 6 is valid or not, we further examine the variance of 6-hourly zonal wind during different phases of the MJO, separately during its active and inactive months. Because MJO active and inactive months tend to occur during QBO easterlies and westerlies respectively, which are also expected to influence stratospheric waves, only MJO events during the QBON phase are analyzed and are shown in Figure 7.

In Figures 7a and 7b, shading is the variance of zonal wind anomalies for active and inactive MJO months respectively, however, for Figure 7c, shading is the difference between variance of zonal wind anomalies for active and inactive MJO months, during QBON; positive shading (red) represents the higher variance of zonal wind anomalies for active MJO months and negative shading (blue) represents the lower variance of the zonal wind anomalies for active MJO months associated with the interannual time scale. From Figures 7a and 7b, it is clear that there is a higher variance of the stratospheric waves for Phases 1, 4, 5, and 8 during active than inactive MJO months when QBO is neutral, which is depicted even clearer in Figure 7c. Hence, Figure 7 suggests that there is a presence of higher variance or higher activities of the stratospheric waves to all OMI Phases during active MJO months than inactive MJO months. This result suggests that there might be an underlying dynamical mechanism that relates the activities of active MJO in the troposphere with the higher activities of the waves in the stratosphere i.e., around 10 hPa.

These results we have shown in section 3.1 still need to do significant testing and will be one of our future works. Even though these results show that there are higher activities of the stratospheric waves during active MJO months, it is still unclear which exact stratospheric waves might be influenced by the MJO. Therefore, in the next chapter, we will use power spectral analysis to evaluate how different types of stratospheric waves vary with monthly MJO activities.

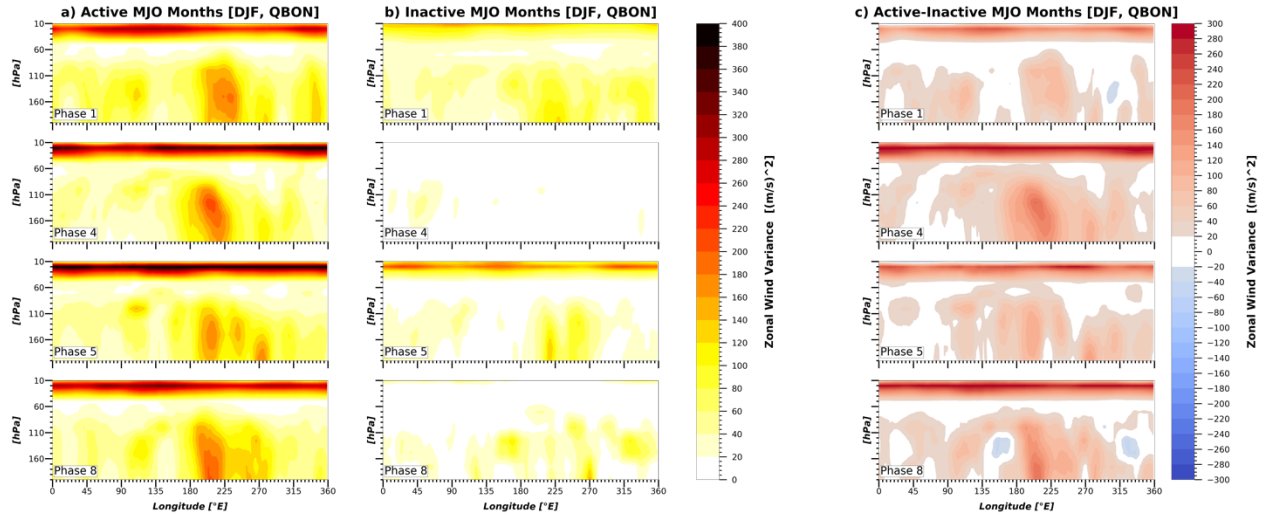


Figure 7: Longitude height cross-section of composites of the evolution of stratospheric wave for QBON months associated during different MJO phases 1, 4, 5, and 8, respectively from top to bottom for boreal winter: (a) For Active MJO months, (b) For Inactive MJO months and (c) For the difference of active and inactive MJO months. Color shading is a 120-days filtered zonal wind anomaly variance.

3.2 Power Spectrum Analysis

To evaluate stratospheric wave activity with monthly QBO and OMI indices, we first generate monthly time series of power spectra by following the method of M. Wheeler & Kiladis, (1999). We apply the wavenumber-frequency Fourier Transform technique to ERA-I and ERA-5 zonal wind anomalies at 50 hPa between 15°N and 15°S with a 96-days window centered on the 15th of each month, producing monthly time-series of wavenumber-frequency power spectra. The 96-days window is selected to capture sub-seasonal convective activities. For each window, a temporal linear trend is removed and the beginning and ending 10% of the data are tapered to zero using a Hanning window.

We use both ERA-I and ERA5 to check the presence of any kind of association between monthly MJO activities with stratospheric waves. Both ERA-I and ERA5 have sufficient resolution in horizontal and temporal scales to diagnose the synoptic-scale stratospheric waves that are known to drive the QBO through their associated vertical momentum fluxes. However, ERA5 has higher spatial and temporal resolutions, and these improved resolutions of ERA5 relative to ERA-I benefit a better representation of convective updrafts, gravity waves, tropical cyclones, and other meso to synoptic-scale atmospheric features (Hersbach et al., 2020; Hoffmann et al., 2019).

The main merit of using ERA5 data over ERA-I in this study is due to its ability to detect high-frequency gravity waves and to check the sensitivity of our results to the choice of reanalysis data.

The monthly power spectra that we create are for symmetric and antisymmetric parts. The symmetric signal is defined as the average zonal wind anomalies at the same degrees of latitude to the north and south of the equator, capturing the symmetric structure (same sign anomalies) about the equator. The antisymmetric signal is defined as the difference in zonal wind anomalies at the same degrees of latitude north and south of the equator, capturing the antisymmetric structure (opposite sign anomalies) about the equator (M. Wheeler & Kiladis, 1999). These techniques are commonly used to separate different modes of equatorial waves whose structure can be characterized as symmetric and antisymmetric about the equator. We calculate the climatology of each symmetric and antisymmetric monthly power spectra in the time dimension and then take an average of them to generate background monthly power spectra which we smooth on wavenumber and frequency dimensions 100 times. After that, each of the symmetric and antisymmetric monthly power spectra is divided by the background which is smoothed 100 times to calculate the climatological power spectrum for the symmetric and antisymmetric parts, which will be referred to as normalized power spectra.

Shading is the normalized power of zonal wind anomaly, where higher values indicate higher activities of the stratospheric waves in Figures 8 and 9. Figures 8a and 8b show the climatological of symmetric and antisymmetric power spectrum at 50 hPa from ERA-I. There are higher values of normalized power spectra in the region of equatorially trapped Kelvin wave and Mixed Rossby Gravity (MRG) waves for symmetric and anti-symmetric power spectrum respectively. We also detect Westward Inertia Gravity (WIG) and Equatorial Rossby (ER) waves in symmetric parts.

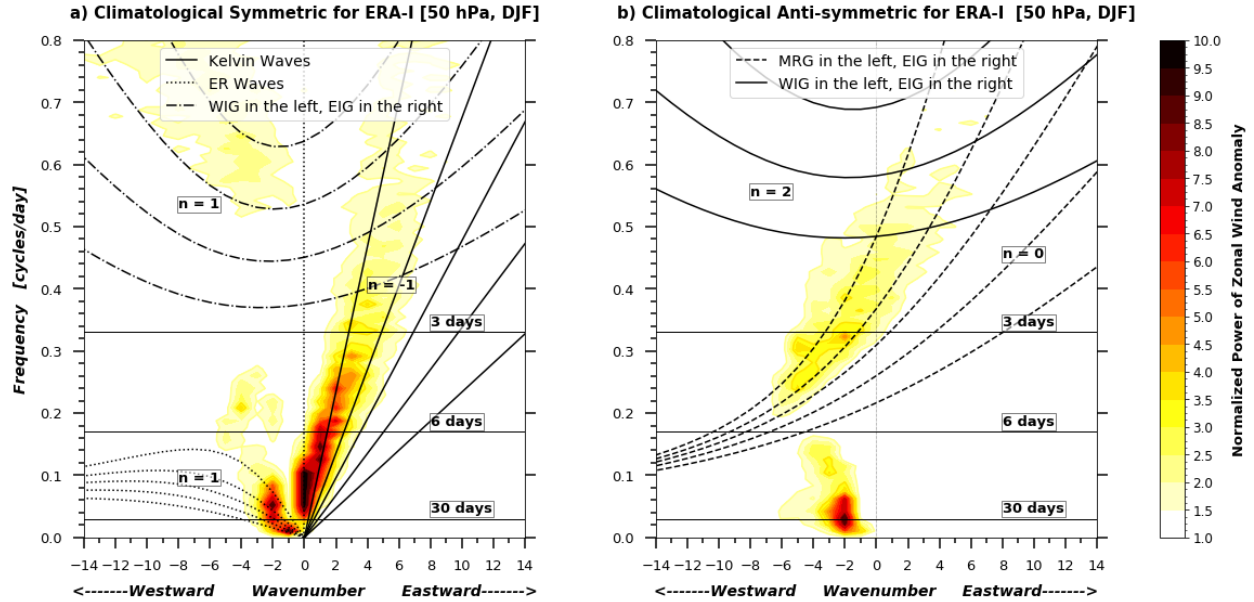


Figure 8: Climatological power spectrum for ERA-I at 50 hPa with overlaid dispersion curve with an equivalent depth of 300m, 100m, 50m, 25m, and 12m; (a) For symmetric part consisting of Kelvin, Equatorial-Rossby (ER) and Westward Inertia Gravity (WIG)/Eastward In Inertia Gravity (EIG) waves denoted by solid, dotted and dashed-and-dotted lines with meridional mode numbers (n) -1 , 1 and 1 respectively. Dashed-and-dotted line with $n = -1$ in the left is for WIG and in the right is for EIG. (b) For antisymmetric part consisting of Mixed Rossby-Gravity (MRG), Eastward Inertia Gravity, and Westward Inertial Gravity Waves denoted by dashed and solid lines. The dashed line with $n = 0$, in the left, is for MRG and in the right for EIG, on the other hand, a solid line with $n = 2$, in the left is for WIG, and in the left is for EIG. Shading represents the normalized power of zonal wind anomaly.

Figures 9a and 9b show climatology of the symmetric and antisymmetric power spectrum at 50 hPa for ERA5 respectively. And, like ERA-I, ERA5 captures equatorially trapped Kelvin, MRG, WIG, and ER waves. In both Figures 8 and 9, it is seen that there is the presence of higher activities of Kelvin, WIG, and ER waves for symmetric and MRG wave for the antisymmetric part. Conclusively, Figures 8 and 9 show that both ERA-I and ERA5 can capture Kelvin, WIG, and ER waves for symmetric and MRG waves for antisymmetric power spectra. Among which Kelvin and MRG waves play very important roles in the modulation of the dynamics of the QBO and have been demonstrated in prior studies too (Baldwin et al., 2001a; Dunkerton, 1997; Pahlavan, Fu, et al., 2021; Pahlavan, Wallace, et al., 2021). It is also to be noticed, all these waves in ERA5 are shallower which is detected by a small shift in their equivalent depth represented by the dispersion curves as compared to the ERA-I. However, for this research, this shift doesn't play a vital role in the analysis.

To further evaluate how the power spectra change with the QBO and MJO activity, we quantify anomalous monthly time-series of power spectra by removing its seasonal cycle at each resolved wavenumber and frequency. As done in the previous chapters, we remove the time-mean and the first three harmonics of the seasonal cycle to generate anomalies. The anomalous time-series of power spectra are then further normalized using their standard deviation at each resolved wavenumber and frequency. To check if the reanalysis captures the expected variability of stratospheric wave activity with the QBO, this monthly time series of the normalized power spectra are regressed onto the monthly QBO index at 50-hPa described in section 2.4.

Figures 10 and 11 show the resultant regression coefficients of the power spectrum at 50 hPa for ERA-I and ERA5, respectively. Negative coefficients (blue shading) indicate that the power decreases during QBO westerly and increases during QBOE, while the reverse is true for positive coefficients (red shading). Figures 10a and 11a show that Kelvin wave activity is higher during QBOE months, while Figures 10b and 11b show that MRG wave activity is higher

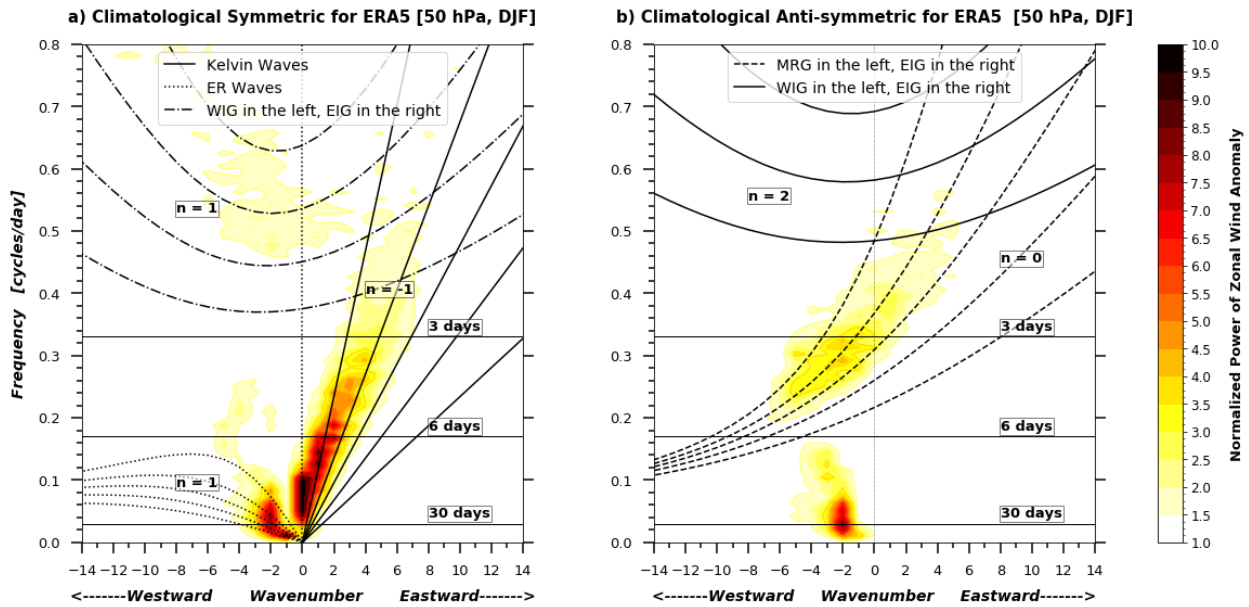


Figure 9: Same as Figure 8 but for ERA5.

during QBOW months. In addition, both signals are significant at a 97.5% confidence level for both Figures 10 and 11. This finding is consistent with previous work depicting more Kelvin wave activities during QBOE months and more MRG wave activities during QBOW months (Baldwin et al., 2001a; Pahlavan, Fu, et al., 2021; Pahlavan, Wallace, et al., 2021).

Besides Kelvin and MRG waves, we also can see higher activities of Westward Inertia-Gravity (WIG) of $n = 1$ & 2 , Equatorial Rossby (ER) waves of $n = 1$ waves during QBOW months as seen in Figures 10 and 11. On the other hand, stratospheric waves such as WIG and ER during QBOW months have more activities for different wavenumbers when ERA5 is used which is not the case for ERA-I. And this clear distinction might be due to the higher resolution of ERA5 over ERA-I.

Figures 10 and 11 demonstrate that both reanalyses capture the expected variability of stratospheric wave activity associated with the QBO. In addition, it also shows that the monthly activity of stratospheric waves is strongly influenced by the QBO. Therefore, to evaluate how the MJO might influence the stratospheric wave activity, we first need to remove its monthly variability associated with the QBO. As done in Chapter 2, we eliminate the QBO signal by using the regression model to reconstruct the normalized monthly power spectrum anomalies that are linearly associated with the QBO and remove them. The remaining normalized monthly power spectrum anomalies are then linearly regressed onto the monthly OMI amplitude.

Figures 12 and 13 show the regression coefficients of such power spectra regressed onto the monthly OMI. And it is limpid from Figures 12 and 13, no statistically significant normalized power of stratospheric waves appears to be linearly related to the monthly OMI. We also apply the same analysis for other levels such as 200 hPa, 100 hPa, 70 hPa, 30 hPa, 20 hPa, and 10 hPa for ERA-I and 200 hPa, 175 hPa, 150 hPa, 125 hPa, 100 hPa, 70 hPa, 30 hPa, 20 hPa and 10 hPa for ERA5 to check if we can see any stratospheric waves being linearly modulated by the MJO, however, we are not able to find any valid evidence (not shown). These results suggest that there is no linear association between monthly MJO activities and stratospheric waves.

So far, we find no linear association between the monthly activity of the MJO and higher frequency stratospheric wave activity, but in our previous section 3.1, we find the presence of higher activities of stratospheric waves represented by higher values of variance of zonal wind anomalies for active MJO months, suggesting the possible impact of the active MJO activities on the stratospheric waves. That's why we also investigate the non-linear association between the MJO and stratospheric waves. We examined the composites of power spectra during active and inactive MJO months during each QBOE, QBOW, and QBON phase separately. We then normalize each climatology by background power spectra which are smoothed 100 times for each level mentioned earlier for ERA-I and ERA5 and plot. However, we still did not find a significant

relationship between the monthly MJO activities and stratospheric waves (not shown here). Thus, these results suggest two possible interpretations:

- a) The result we found is true and there are no significant impacts of the monthly MJO activities on the activity of stratospheric waves and the dynamics of the QBO.
- b) Or the ERA reanalysis data are not sufficient to resolve high-frequency gravity waves that may still be influenced by the MJO.

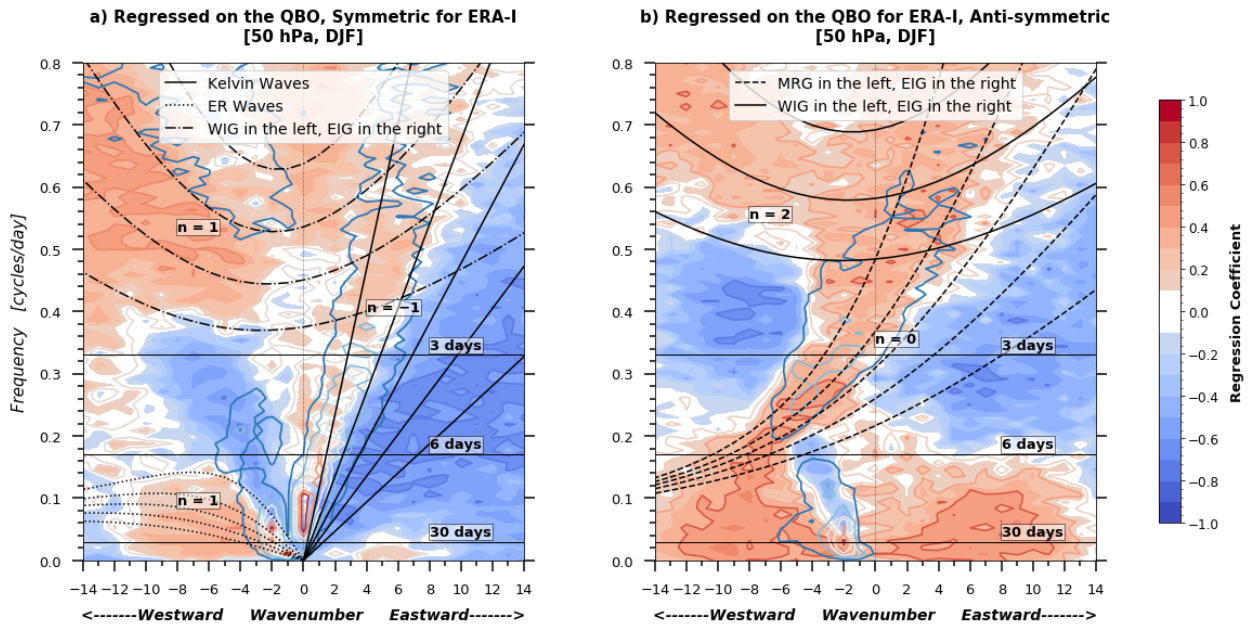


Figure 10: Regressed power spectrum for ERA-I at 50 hPa with overlaid dispersion curve with the equivalent depth of 300m, 100m, 50m, 25m, and 12m; (a) For symmetric part consisting of Kelvin, ER, and WIG/Eastward Inertia Gravity (EIG) waves denoted by solid, dotted and dashed-and-dotted lines with meridional mode numbers (n) -1 , 1 and 1 respectively. Dashed-and-dotted line with $n = -1$ in the left is for WIG and in the right is for EIG. (b) For antisymmetric part consisting of MRG, Eastward Inertia Gravity, and WIG-waves denoted by dashed and solid lines. The dashed line with $n = 0$, in the left, is for MRG and in the right for Eastward Inertia Gravity, on the other hand, a solid line with $n = 2$, in the left is for WIG, and in the left is for Eastward Inertia Gravity. Shading is the regression coefficient. Contours show the normalized power of zonal wind anomalies.

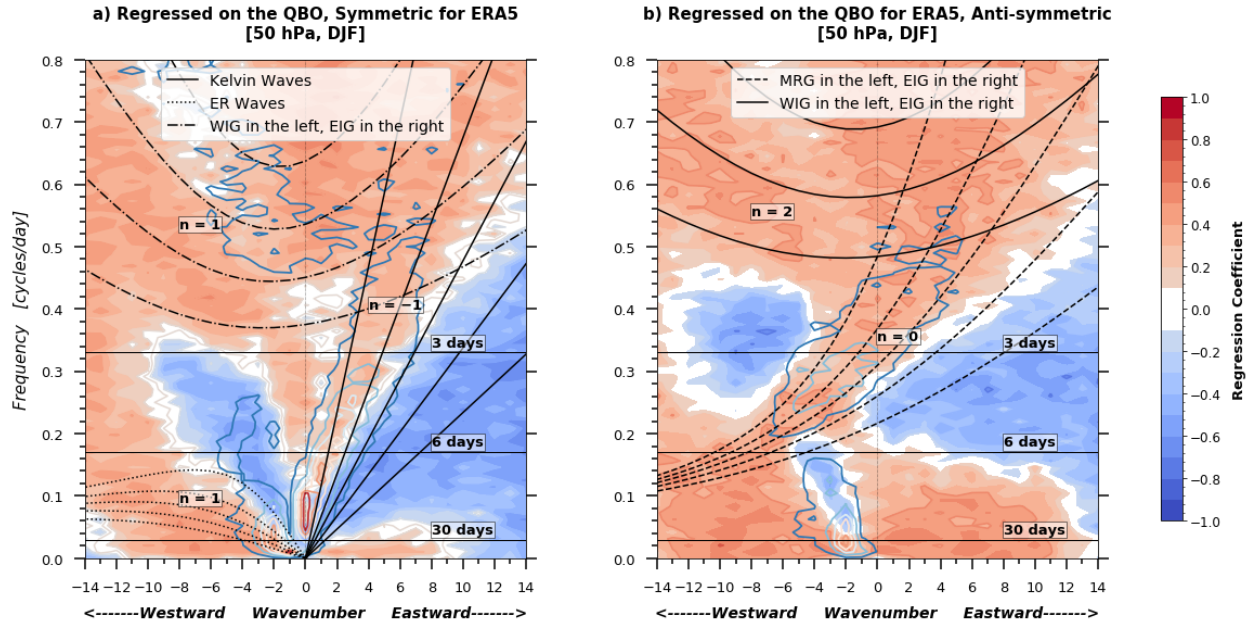


Figure 11: Same as Figure 10, but for ERA5.

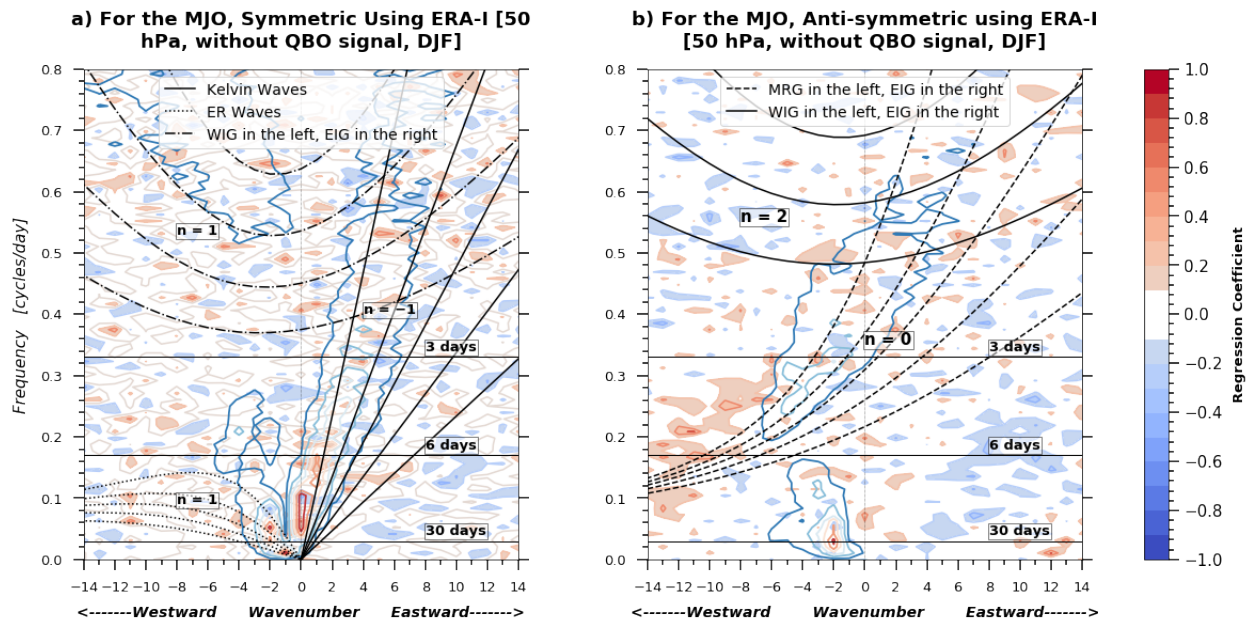


Figure 12: Same as Figure 10 but for MJO months after removing the QBO related linear signal.

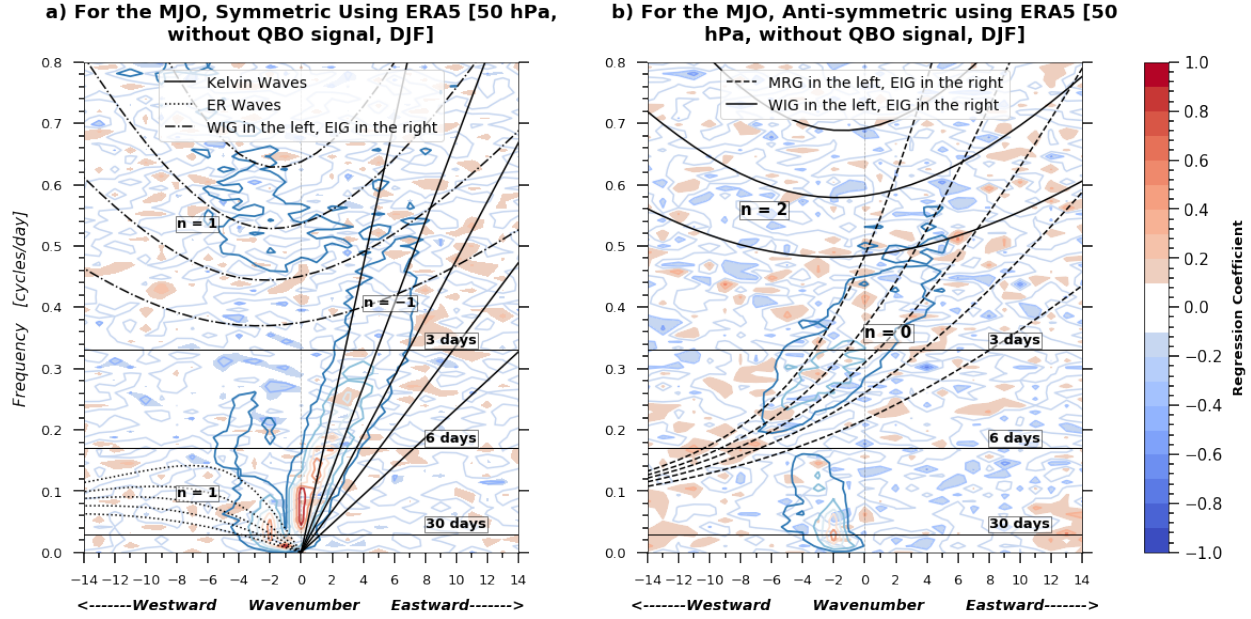


Figure 13: Same as Figure 11 but for MJO months after removing the QBO related linear signal.

3.3 Combined Effects of the QBO and the MJO on Stratospheric Waves

To further examine the potential non-linear impacts of the MJO on stratospheric waves, we evaluate and analyze the combined impacts of the MJO and the QBO on the activity of the stratospheric Kelvin, ER, and MRG waves. To do so, we identify the monthly activity of Kelvin, ER, and MRG waves by averaging the power spectra over a specific range of frequency and wavenumber corresponding to Kelvin (i.e., $0 \leq \text{wavenumber} \leq 10$; $0 \leq \text{frequency} \leq 0.5$), ER (i.e., $-9 \leq \text{wavenumber} \leq -2.5$; $0 \leq \text{frequency} \leq 0.08$) waves on symmetric and MRG (i.e., $-8 \leq \text{wavenumber} \leq -1$; $0.18 \leq \text{frequency} \leq 0.25$) on the antisymmetric monthly power spectrum of ERA-I and ERA5. These resultant monthly time series of power spectra represent the monthly activity of each wave, which are then composited based on monthly OMI and QBO indices described in sections 2.1 and 2.4 respectively.

In Figures 14 and 15, higher values (red shading) represent higher activities and lower values (blue shading) represent lower activities of the specific wave. In general, the activity of all Kelvin, ER, and MRG waves is strongly dependent on the QBO, which is consistent with Figures 10 and 11. However, Figures 14a and 15a suggest that Kelvin wave activities are slightly being modulated by the monthly MJO activities as indicated by the subtle change in the values of power

when QBO is easterly for boreal winter months. In other words, when the QBO is in its easterly phase, we notice the increase in monthly activities of Kelvin wave with the active than the inactive MJO months for boreal winters. ER and MRG waves activities, on the other hand, are found to have been slightly modulated by the monthly MJO activities just like Kelvin wave but when the QBO is in its westerly phase for boreal winter months as shown in Figures 14b and 15b, and Figures 14c and 15c, respectively. In a nutshell, we find during the QBOW phase, increments in the activities of ER and MRG waves, and during the QBOE phase, increments in Kelvin wave activities, are directly proportional to the MJO active months.

In conclusion, while analyzing the combined impacts of the MJO and the QBO on different stratospheric waves such as Kelvin, ER, and MRG by using reanalyses data, we detect very subtle non-linear dependency of these stratospheric waves on the monthly MJO activities which was not identified when power spectral analysis described in section 3.2 was implemented. Even though the QBO has a strong influence on the activities of stratospheric Kelvin, ER, and MRG waves in general, the results here suggest the possibility of a subtle influence of the MJO activities on stratospheric wave activities. However, the significance testing of this result is yet to be done and we will be doing it in the future.

So far, all results we present in this paper are based on reanalysis data which has its pros and cons. Even though we have used highly resolved ERA5 data, we still are unable to capture any significant impacts of the MJO activities on the synoptic-scale stratospheric wave activities. We, nevertheless, do get results hinting slight impact of monthly MJO activities on stratospheric waves like Kelvin, ER, and MRG, the significance is yet to be tested as stated earlier. Our analysis so far is also limited to examining the variability of synoptic-scale stratospheric waves. There is a possibility that the MJO may influence stratospheric waves on timescales shorter than a day i.e., high-frequency (period shorter than a day) stratospheric wave, which is yet to be analyzed because of the accurate representation of such high-frequency waves by the reanalyses is questionable. Therefore, in our next chapter, to further understand stratospheric wave dynamics and their relationship with the MJO activities and the QBO dynamics, we are shifting to observational data that can capture high-frequency waves.

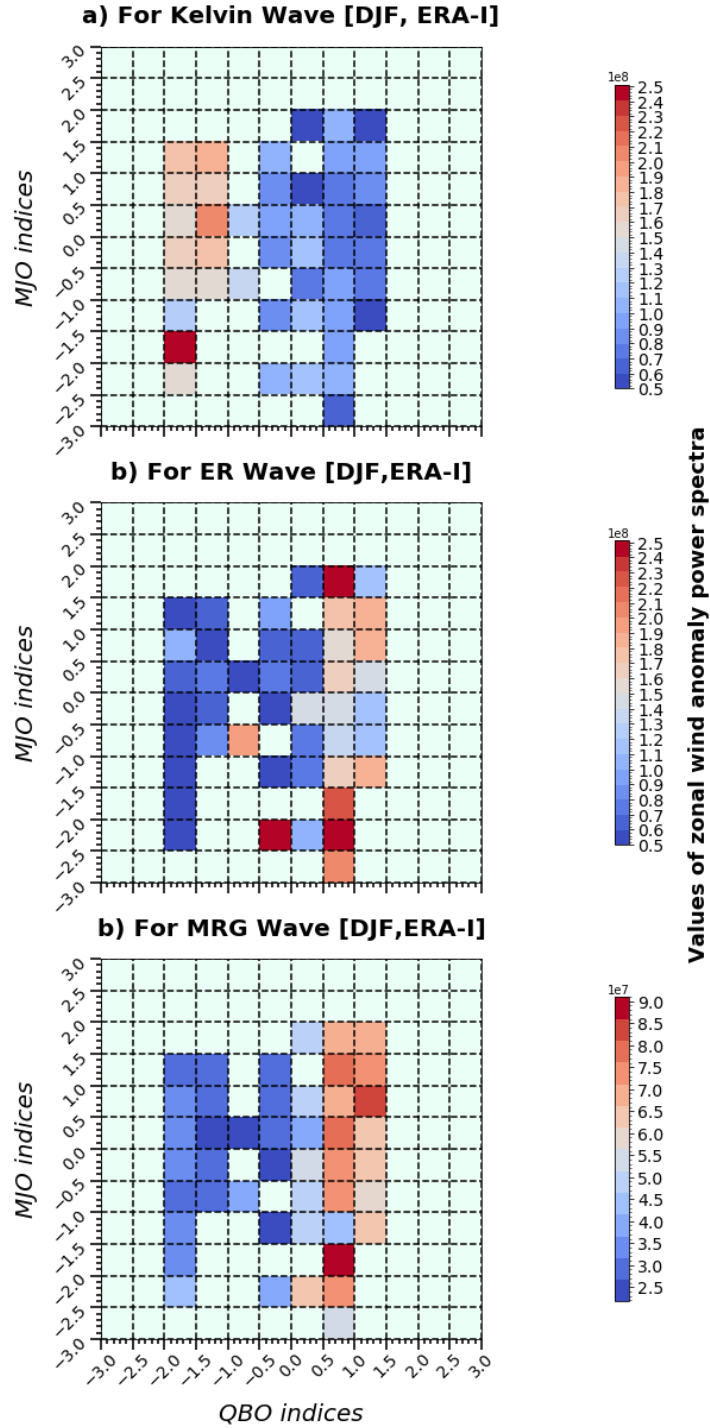


Figure 14: Combined impacts of the MJO and the QBO on stratospheric waves based on ERA-I; (a) For Kelvin Wave, (b) For ER Wave, and (c) For MRG Wave. Shading shows the composites of monthly power of zonal wind anomaly at each QBO and MJO bin for boreal winter.

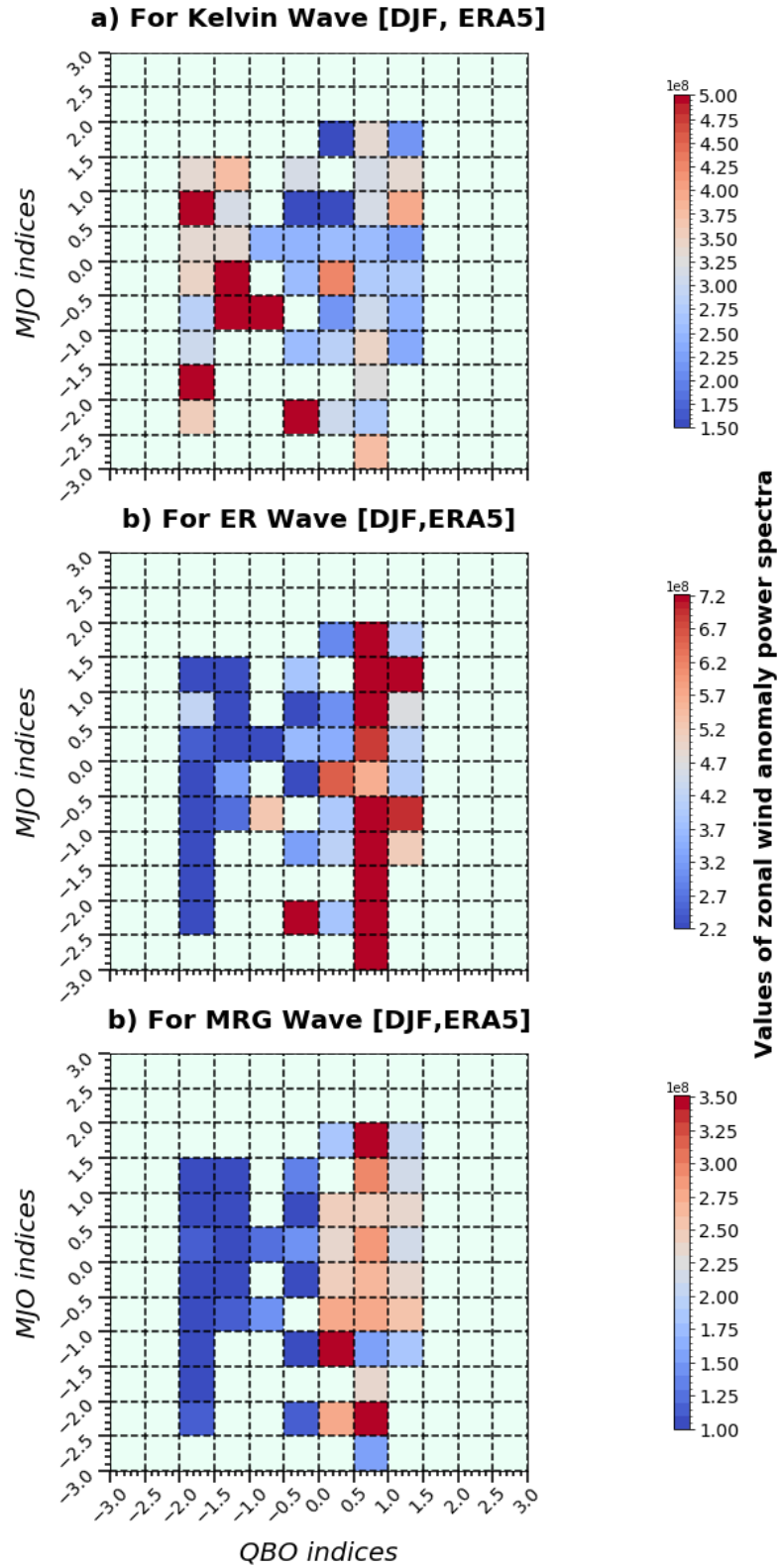


Figure 15: Same as Figure 14 but for ERA5.

4 Re-evaluation of the Stratospheric Wave Activity using Radar Observational Data

The main objective of this chapter is to reinvestigate the activity of stratospheric waves using radar observational data from the Equatorial Atmosphere Radar (EAR) provided collaboratively by the Research Institute for Sustainable Humanosphere (RISH), Kyoto University, and National Institute of Aeronautics and Space of Indonesia (LAPAN). The EAR is a large Doppler radar built for atmospheric observation at the equator in West Sumatra in the Republic of Indonesia. The configuration system in the EAR helps to control frequency up to 5000 times per second. And it consists of a circular antenna array which is an active phased array system with 560 three-element Yagis. Meanwhile, it is highly resolved with a vertical resolution of 0.15 km from the surface in the troposphere to 20 km in the lower-stratosphere and has a temporal resolution of 10 minutes. This high temporal and vertical resolution of the data allows us to examine the potential impact of the MJO on waves with periods shorter than a day. We have used EAR data from 2002 to 2017 and focus on the layer above 15 km (near the tropopause and above) for this chapter of our analysis.

To re-evaluate the activity of stratospheric waves with monthly OMI and QBO indices, as done with ERA-I and ERA5, we first generate monthly time series of power spectra by following the method illustrated in M. Wheeler & Kiladis, (1999). However, because EAR data is only available at one location, we apply the 1-D Fast Fourier technique to EAR zonal wind anomalies with a 96-days window centered on the 15th of each month, producing monthly time series of resolved frequency power spectra for different heights at and above 15 km. Although this data does not provide any information about the wavenumber and propagation direction of stratospheric waves, it allows us to examine high-frequency stratospheric waves that are not possible with the reanalyses.

Figure 16a shows the climatological power spectrum for all winter months, depicting that there is generally a uniform amount of activity at all frequencies between 15 and 19.6 km, with some higher activities found at a frequency of 2.62 cycles/hour (period of ~23 minutes). And this power at 2.62 cycles/hour is as comparable in the lower stratosphere as it is seen in the upper troposphere. Figure 16b shows the difference in the power spectra during QBOE and QBOW months. In Figure 16b, positive (red) shading represents higher activities of waves during QBOE months, and negative (blue) shading represents higher activities of waves during QBOW months.

It shows that there is a higher activity of waves throughout the upper troposphere and lower stratosphere (UTLS) during an easterly phase of the QBO and the reverse is true for the westerly phase of the QBO. The difference in the power between QBOE and QBOW maximizes at around 19.6 km (~50 hPa) where the QBO phases are defined. In summary, Figure 16 suggests that there are higher activities of high-frequency gravity waves in the UTLS layer during the QBO easterly phase as compared to QBO westerly phase. And this result is significant at a 95% confidence level when performing a Monte-Carlo resampling test using 1000 iterations with repetitions.

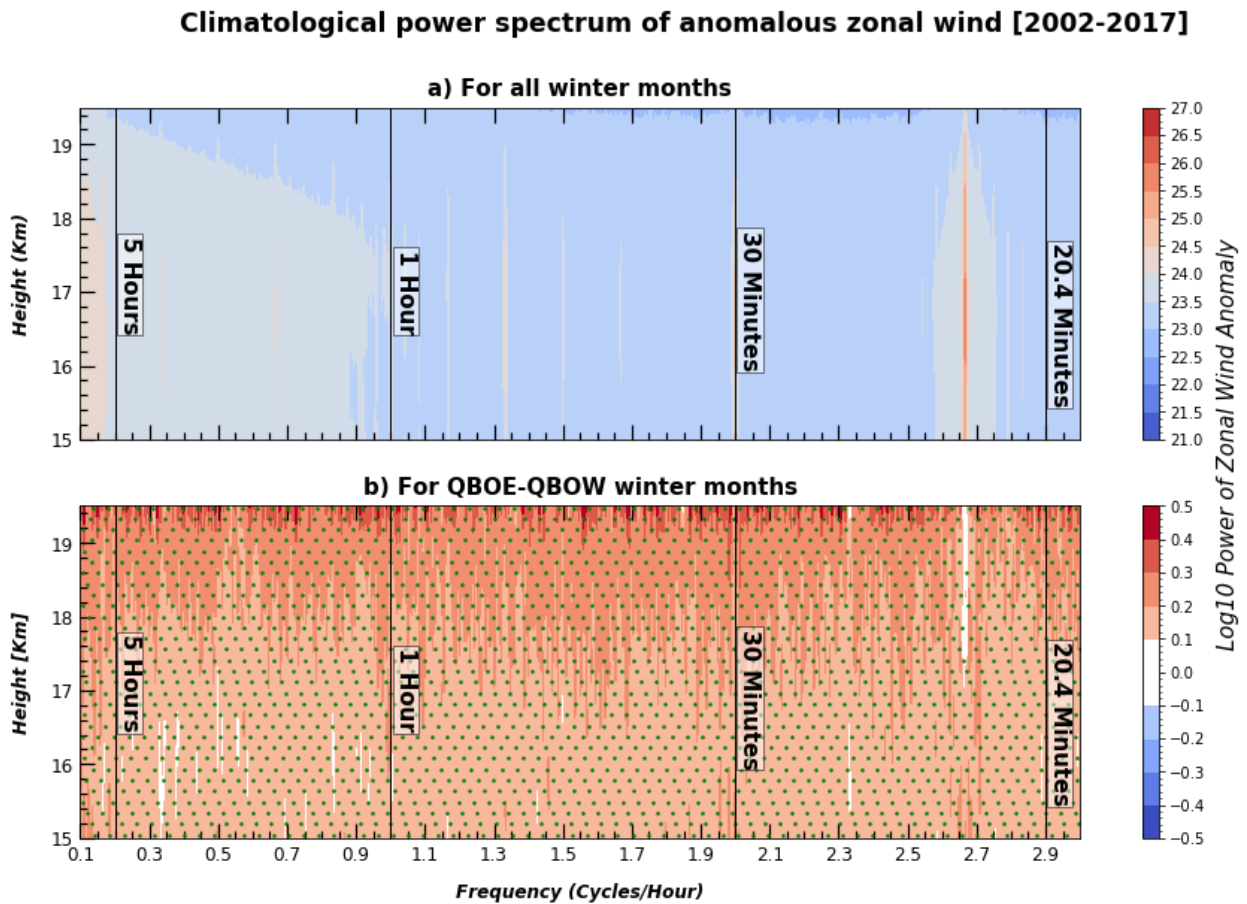


Figure 16: Climatological power spectrum of zonal wind anomaly for all boreal winter months from 2002-2017; a) For all winter months, and (b) For the difference between QBOE and QBOW months. Shading is the climatological base10 logarithmic values of monthly power of zonal wind anomalies. Green dots represent the region of 95% confidence level in Figure 16b.

Furthermore, we evaluate how the power spectra change with the QBO and MJO activity as done in section 3.2. We quantify anomalous monthly power spectra by removing its seasonal

cycle at each resolved frequency by removing the time-mean and the first harmonic of the seasonal cycle and normalizing by their standard deviation at each resolved frequency. To further analyze the variability of stratospheric waves obtained by using observational radar data, with the activity of the QBO, this monthly time-series of the normalized power spectra are regressed onto the monthly QBO index at 50 hPa as described in section 2.4 only for boreal winter and is shown in Figure 17.

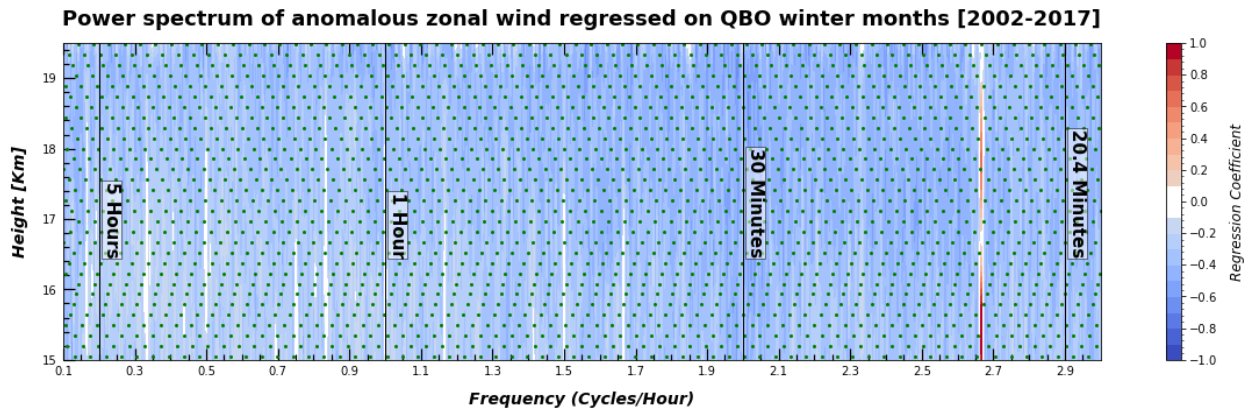


Figure 17: Power spectrum of zonal wind anomaly regressed on the monthly QBO indices at 50 hPa for boreal winter from 2002-2017. Shading is the values of regression coefficients between monthly normalized power of zonal wind anomaly and QBO–Index for boreal winter months. Green dots represent the region of 95% confidence level.

Figure 17 shows the vertical cross-sections of the regressed coefficients of the power spectrum. Negative coefficients (blue shading) indicate that the activity of waves increases during QBOE months and decreases during QBOW months, while the opposite is true for positive coefficients (red shading) as stated earlier. Figure 17 indicates that there are higher activities of stratospheric waves in UTLS at all frequencies during the QBO easterly phase, consistent with the results shown in Figure 16b. To then examine MJO impacts on stratospheric waves activities, as done in section 3.2, we first eliminate the QBO signal by using the regression model to reconstruct the monthly power spectrum anomalies that are linearly associated with the QBO from monthly normalized power spectra. Thus, the remaining monthly power spectrum anomalies are then regressed onto the monthly OMI for boreal winter months and are depicted in Figure 18.

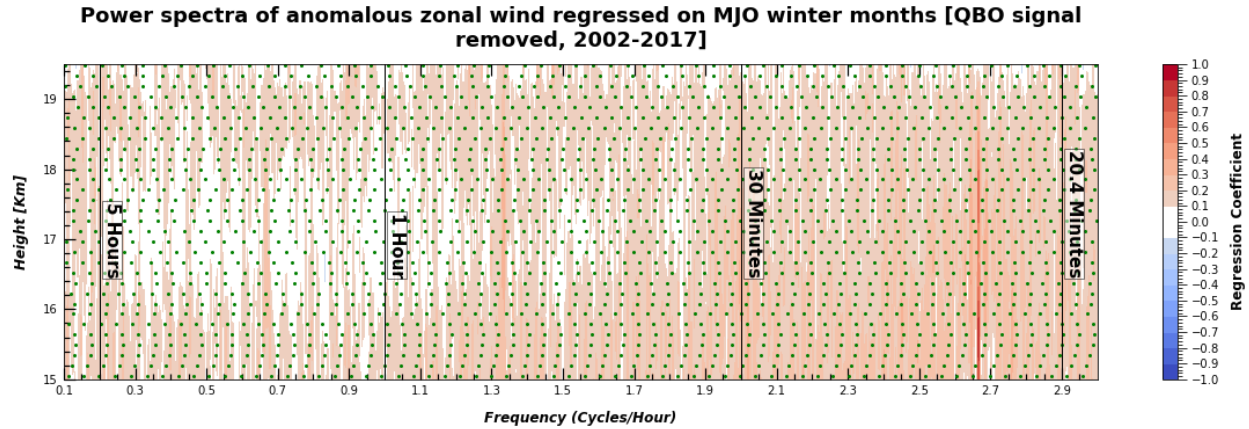


Figure 18: Power spectrum of zonal wind anomaly after removing QBO signal, regressed on monthly OMI at 50 hPa for boreal winter from 2002 to 2017. Shading is the regression coefficients between monthly normalized power of zonal wind anomaly after removing QBO signal and monthly OMI, for boreal winters only. Green dots represent the region of a 95% confidence level.

In Figure 18, positive (red) shading represents higher activities of the high-frequency zonal wind anomalies during active MJO months, and negative (blue) shading represents lower activities of the high-frequency zonal wind anomalies during active MJO months. While analyzing Figure 18 it is seen that most of the regions above 15 km have higher activities of high-frequency zonal wind anomaly when the monthly MJO is active. On the other hand, just as in Figure 17, in Figure 18, we detect higher activities of waves at 2.62 cycles/hour (~23 minutes) persistent throughout the upper troposphere till the lower stratosphere during active MJO months and shows the tendency of high-frequency gravity waves generated in the troposphere to impact up till lower stratosphere when there is the presence of active MJO activities. Overall Figure 18 advocates the subtle presence of higher activities of high-frequency stratospheric waves linearly associated with the active monthly MJO activities in the troposphere represented by red shading.

Knowing the result from Figure 18 is not adequate to build a base confirming the influence of active MJO activities on the stratospheric wave activities, we inspect how the high-frequency waves above 15 km change non-linearly during active and inactive MJO months after the removal of linear signals associated with the QBO from monthly normalized power spectrum anomalies. For that, we calculate a composite of remaining monthly power spectrum anomalies when the MJO is active and inactive based on monthly OMI as described in section 2.1 and is represented in Figure 19.

In Figure 19, the red shading represents higher activities, and the blue shading represents lower activities of high-frequency zonal wind anomaly during active MJO months. In Figures 19a

and 19b, the power is mostly negative i.e., blue shading, representing lower activities of the high-frequency stratospheric waves associated with the active and inactive monthly MJO activities. These results from Figures 19a and 19 b, suggest that primarily high-frequency stratospheric waves are not non-linearly modulated by the monthly MJO activities. However, we capture the tentative higher activities of the high-frequency stratospheric waves during active than inactive MJO months which is even clearly illustrated in Figure 19c with statistical significance at the 95% confidence level in most of the region. Figures 18 and 19 together characterize the presence of higher activities of the high-frequency stratospheric waves mostly during active MJO months. In conclusion, even though there are some differences between the regression and composite analyses, both results show that there are higher high-frequency stratospheric waves activities during active rather than inactive MJO months in the lower stratosphere.

The results of this chapter and previous chapters indicate that the MJO mainly influences high-frequency stratospheric waves (periods shorter than a day) that could not be captured using reanalyses data. Therefore, the subtle relationship between the MJO activity and downward propagation speed of the QBO shown in Chapter 1 may be driven by the MJO influence on the high-frequency stratospheric waves and their associated momentum fluxes, which needs to get investigated.

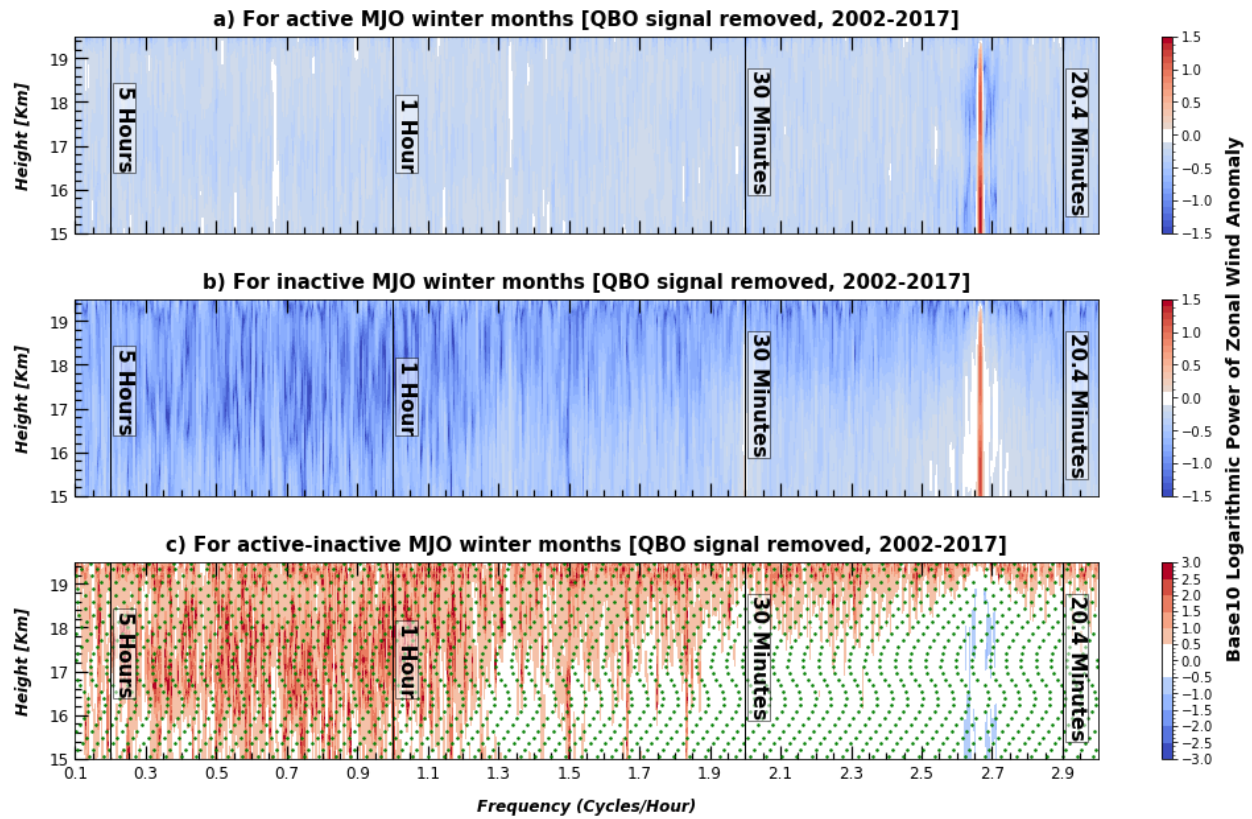


Figure 19: Composites of normalized monthly power spectrum after removing linear signals associated with the QBO, (a) For active MJO months, (b) For inactive MJO months, and (c) Difference between active and inactive MJO months, during boreal winter only. Green dots elucidate the region of a 95% confidence interval in Figure 19c.

5 Summary

5.1 *Review of motivations and methods*

Previous studies have found that the MJO convection is more active over the warm pools during an easterly phase of the QBO, but the mechanism behind their relationship remains unresolved. Previous studies have hypothesized that change in vertical static stability in the cold tropical tropopause layer is responsible for driving the MJO-QBO relationship, but this mechanism cannot fully explain the observed MJO-QBO relationship. Therefore, this thesis examined an alternative hypothesis: the stratospheric waves generated from MJO convection may influence the QBO by altering the amount of vertical momentum flux, and hence, leading to the known relationship between them. It is known that equatorial waves like Kelvin, Inertia Gravity, MRG, and other small scale gravity waves, generated by tropical convection, are responsible for the dynamics of the QBO in the stratosphere by modulating and providing momentum fluxes and wave forcing (Baldwin et al., 2001b; Dunkerton, 1997; Pahlavan, Fu, et al., 2021; Pahlavan, Wallace, et al., 2021). To test our hypothesis, this study was employed to evaluate and understand the relationship between the MJO and QBO via modulation of the stratospheric waves. In short, they were implemented to provide insight into two questions:

1. Does the MJO influence stratospheric wave activities?
2. If it does, could this be the mechanism driving the documented MJO-QBO relationship?

5.2 *Review of Results*

We, at first re-evaluated the relationship between the MJO and QBO by using the EOF-based QBO Index (Densmore et al., 2019) from 1979 to 2017 for boreal winters only. This method allowed us to quantify the descent rate of the QBO from the upper stratosphere until it dissipates below 50 hPa that cannot be achieved by using a single level QBO index (Son et al., 2017b; Yoo & Son, 2016) as described in section 2.4. As a result, we find a slight and significant positive correlation between the monthly downward propagation speed of the QBO with monthly MJO activities. This result indicates that the westerly phase of the QBO descends faster from the upper stratosphere to the lower stratosphere during active MJO months in the troposphere and vice-versa. Moreover, this result we got is maintained even during the neutral phase of the QBO when there is no impact of the QBO in its descent rate. While the result we got for the OMI shows the faster

downward propagation speed of the QBO associated with monthly MJO activities, it was not found when the RMM index was used. That is why this result is not sufficient enough to claim the modulation of the QBO dynamics by tropical MJO activities, and we shifted to power spectral analysis.

Secondly, to evaluate stratospheric wave activity with monthly QBO and OMI indices, we used power spectral analysis by following the method of M. Wheeler & Kiladis, (1999). And this power spectral analysis of ERA-I and ERA5 zonal wind anomaly at 50 hPa showed that there are higher Kelvin wave activities during the QBOE phase and higher MRG waves during the QBOW phase as suggested by previous studies (Densmore et al., 2019; Marshall et al., 2017; Nishimoto & Yoden, 2017b; Son et al., 2017b; Zhang & Zhang, 2018). These results indicated that reanalyses sufficiently capture the interannual variability of stratospheric waves associated with the QBO. However, we found no specific signal of any stratospheric waves associated with monthly MJO activities in both ERA-I and ERA5. We have detected a subtle non-linear dependency of Kelvin, ER, and MRG waves on monthly MJO activities during certain states of the QBO, but the significance of this result is yet to be tested. Hence, in summary, reanalyses didn't detect any significant signals of stratospheric waves linearly associated with monthly MJO activity but detected subtle non-linear dependency.

To further examine the potential impact of the MJO on high-frequency (period shorter than a day) stratospheric gravity waves that cannot be assessed using reanalyses, we used radar observational data (EAR data) located over Sumatra Island, which is highly resolved in temporal and vertical dimensions up to 19.5 km in altitude. And in a result, we found that high-frequency stratospheric wave activities are higher during the QBOE phase than the QBOW phase. We also analyzed the linear association of the monthly MJO activities with high-frequency stratospheric waves after removing the QBO signal and found some influence of the active MJO activities on high-frequency stratospheric waves. We did analyze the non-linear association of the MJO activities and high-frequency stratospheric gravity waves and found that the activities of high-frequency stratospheric waves are somewhat non-linearly modulated by active MJO months. These results suggest that active MJO modulates the high-frequency stratospheric waves both linearly and non-linearly which we didn't find while using reanalyses. And the results of the EAR are significant at a 95% confidence level.

Hence, even though monthly MJO activities tend to modulate high-frequency waves as captured from EAR, it is seen from the reanalyses that the tropospheric MJO doesn't influence the activities of the synoptic-scale stratospheric waves either linearly or non-linearly which refute our hypothesis that the modulation of the stratospheric waves and associated momentum fluxes by the MJO drive the observed relationship between the MJO and the QBO. This finding suggests the lack of role of the MJO activities on modulating the dynamics of the QBO via synoptic-scale stratospheric wave forcing. Although we found no significant role of the MJO activities in modulating the dynamics of the QBO through synoptic-scale stratospheric waves, this research is still important as it helped to better understand the dynamics of the MJO-QBO relationship to a greater extent by eliminating one of the possible mechanisms behind their relationship i.e., the tropospheric MJO influencing the dynamics of the stratospheric QBO via stratospheric wave forcing.

Also noting, we hypothesized the modulation of the stratospheric waves and associated momentum fluxes by the MJO drive the observed relationship between the MJO and the QBO, but so far, we have examined only the stratospheric wave forcing (synoptic-scale and shorter scale) associated with the MJO activities. Calculation of the vertical momentum fluxes associated with those waves and their possible impacts on the dynamics of the QBO is yet to be done.

5.3 Caveats and Recommendations for Future Work

Knowing the relationship between the MJO and the QBO exists during boreal winter only as proved by previous studies (Liu et al., 2014; Sakaeda et al., 2020; Yoo & Son, 2016), we mainly focused our study during that period of the year. However, vertical momentum fluxes from high frequencies waves generated by tropical deep convection; responsible to provide forcing for the dynamics of the QBO, are most likely to penetrate tropopause and reach the stratosphere with some time lag between their generation in the tropical atmosphere and penetration in the UTLS regions. In other words, instead of focusing typically on boreal winter, it is comprehensive to extend winter months from November till March to incorporate the impacts of tropical convection related to the MJO in a longer period which we haven't done in this study. This will help to overcome the drawbacks of the time lag between waves generation and their impact in the stratosphere if there are any.

Also, we detect the higher activities of the high-frequency stratospheric waves influenced by active MJO activities unlike synoptic-scale stratospheric waves and the result is significant. Knowing that active MJO activities impact the activities of shorter-scale stratospheric waves, it would be more comprehensive to calculate and analyze vertical momentum fluxes associated with those waves which we haven't done in this research and is going to be one of the future works. The analysis of vertical momentum fluxes associated with stratospheric waves would be helpful to dissect the unexplored but plausible factor in contributing to the modulation of the MJO-QBO relationship

While conducting our analysis, we didn't take account for another possible factor that might contribute to the MJO-QBO relationship such as the role of the cirrus clouds that are formed in the tropical tropopause layer (TTL); known to provide positive radiative feedback on the MJO (Ciesielski et al., 2017; A. del Genio & Chen, 2015), ahead of MJO convection (A. D. del Genio et al., 2012; Virts & Wallace, 2014). Hence, cloud radiative feedback associated with cirrus clouds during MJO convections could be another plausible avenue to dissect the MJO-QBO relationship profoundly and research needs to be done for it.

It is known that there are higher activities of the MJO in the MC and warm pool regions when QBO at 50 hPa is in its easterly phase (Son et al., 2017b; Yoo & Son, 2016). This could also underline that when the MJO is in the MC or warm pool regions i.e., Phases 3, 4, and 5 of the MJO, it tends to produce high-frequency gravity waves that can penetrate UTLS and impacts the dynamics of the QBO. However, in this study, we accounted for all phases of the MJO during boreal winter except for section 3.1, which might impact our results from reanalyses and radar observational data. It could be even more convincing to investigate the MJO-QBO relationship for phases when the MJO is in MC or warm pool regions i.e., Phases 3, 4, and 5 to get clearer ideas of the dynamics associated with their relationship if it is the MJO who is the driver of this relationship, which is going to be our one of the future works.

REFERENCES

- Abhik, S., & Hendon, H. H. (2019). Influence of the QBO on the MJO During Coupled Model Multiweek Forecasts. *Geophysical Research Letters*, *46*(15), 9213–9221. <https://doi.org/10.1029/2019GL083152>
- Ahn, M. S., Kim, D., Sperber, K. R., Kang, I. S., Maloney, E., Waliser, D., & Hendon, H. (2017).

- MJO simulation in CMIP5 climate models: MJO skill metrics and process-oriented diagnosis. *Climate Dynamics*, 49(11–12), 4023–4045. <https://doi.org/10.1007/s00382-017-3558-4>
- Back, S. Y. (2020). *Modeling Evidence of QBO - MJO Connection : A Case Study Geophysical Research Letters*. 1–9. <https://doi.org/10.1029/2020GL089480>
- Baggett, C. F., Barnes, E. A., Maloney, E. D., & Mundhenk, B. D. (2017). Advancing atmospheric river forecasts into subseasonal-to-seasonal time scales. *Geophysical Research Letters*, 44(14), 7528–7536. <https://doi.org/10.1002/2017GL074434>
- Baldwin, M. P., & Dunkerton, T. J. (1999). Propagation of the Arctic Oscillation from the stratosphere to the troposphere. *Journal of Geophysical Research Atmospheres*, 104(D24), 30937–30946. <https://doi.org/10.1029/1999JD900445>
- Barrett, B. S., Carrasco, J. F., & Testino, A. P. (2012). Madden-Julian oscillation (MJO) modulation of atmospheric circulation and Chilean winter precipitation. *Journal of Climate*, 25(5), 1678–1688. <https://doi.org/10.1175/JCLI-D-11-00216.1>
- Cassou, C. (2008). Intraseasonal interaction between the Madden-Julian Oscillation and the North Atlantic Oscillation. *Nature*, 455(7212), 523–527. <https://doi.org/10.1038/nature07286>
- Ciesielski, P. E., Johnson, R. H., Jiang, X., Zhang, Y., & Xie, S. (2017). Relationships between radiation, clouds, and convection during DYNAMO. *Journal of Geophysical Research*, 122(5), 2529–2548. <https://doi.org/10.1002/2016JD025965>
- Densmore, C. R., Sanabia, E. R., & Barrett, B. S. (2019). QBO Influence on MJO Amplitude over the Maritime Continent : Physical Mechanisms and Seasonality. *Monthly Weather Review*, 389–406. <https://doi.org/10.1175/MWR-D-18-0158.1>
- Feng, P. N. (2019). *Modulation of the MJO - Related Teleconnections by the QBO Journal of Geophysical Research : Atmospheres*. 22–33. <https://doi.org/10.1029/2019JD030878>
- Feng, P. N., & Lin, H. (2019). Modulation of the MJO-Related Teleconnections by the QBO. *Journal of Geophysical Research: Atmospheres*, 124(22), 12022–12033. <https://doi.org/10.1029/2019JD030878>
- Fritts, D. C., & Alexander, M. J. (2003). Gravity wave dynamics and effects in the middle atmosphere. *Reviews of Geophysics*, 41(1), 1–64. <https://doi.org/10.1029/2001RG000106>
- Garfinkel, C. I., Benedict, J. J., & Maloney, E. D. (2014). Impact of the MJO on the boreal winter extratropical circulation. *Geophysical Research Letters*, 41(16), 6055–6062. <https://doi.org/10.1002/2014GL061094>
- Garfinkel, C. I., Feldstein, S. B., Waugh, D. W., Yoo, C., & Lee, S. (2012). Observed connection between stratospheric sudden warmings and the Madden-Julian Oscillation. *Geophysical Research Letters*, 39(17), 1–5. <https://doi.org/10.1029/2012GL053144>

- Garfinkel, C. I., Shaw, T. A., Hartmann, D. L., & Waugh, D. W. (2012). Does the Holton-Tan mechanism explain how the quasi-biennial oscillation modulates the Arctic polar vortex? *Journal of the Atmospheric Sciences*, *69*(5), 1713–1733. <https://doi.org/10.1175/JAS-D-11-0209.1>
- Guan, B., Waliser, D. E., Molotch, N. P., Fetzer, E. J., & Neiman, P. J. (2012). Does the Madden-Julian oscillation influence wintertime atmospheric rivers and snowpack in the Sierra Nevada? *Monthly Weather Review*, *140*(2), 325–342. <https://doi.org/10.1175/MWR-D-11-00087.1>
- Hendon, H. H., & Abhik, S. (2018). Differences in Vertical Structure of the Madden-Julian Oscillation Associated With the Quasi-Biennial Oscillation. *Geophysical Research Letters*, *45*(9), 4419–4428. <https://doi.org/10.1029/2018GL077207>
- Hendon, H. H., Zhang, C., & Glick, J. D. (1999). Interannual variation of the Madden-Julian oscillation during austral summer. *Journal of Climate*, *12*(8 PART 2), 2538–2550. [https://doi.org/10.1175/1520-0442\(1999\)012<2538:ivotmj>2.0.co;2](https://doi.org/10.1175/1520-0442(1999)012<2538:ivotmj>2.0.co;2)
- Hoffmann, L., Günther, G., Li, D., Stein, O., Wu, X., Griessbach, S., Heng, Y., Konopka, P., Müller, R., Vogel, B., & Wright, J. S. (2019). From ERA-Interim to ERA5: The considerable impact of ECMWF’s next-generation reanalysis on Lagrangian transport simulations. *Atmospheric Chemistry and Physics*, *19*(5), 3097–3214. <https://doi.org/10.5194/acp-19-3097-2019>
- Hung, M. P., Lin, J. L., Wang, W., Kim, D., Shinoda, T., & Weaver, S. J. (2013). Mjo and convectively coupled equatorial waves simulated by CMIP5 climate models. *Journal of Climate*, *26*(17), 6185–6214. <https://doi.org/10.1175/JCLI-D-12-00541.1>
- Kang, W., & Tziperman, E. (2017). More frequent sudden stratospheric warming events due to enhanced MJO forcing expected in a warmer climate. *Journal of Climate*, *30*(21), 8727–8743. <https://doi.org/10.1175/JCLI-D-17-0044.1>
- Kessler, W. S., & Kleeman, R. (2000). Rectification of the Madden-Julian Oscillation into the ENSO cycle. *Journal of Climate*, *13*(20), 3560–3575. [https://doi.org/10.1175/1520-0442\(2000\)013<3560:ROTMJO>2.0.CO;2](https://doi.org/10.1175/1520-0442(2000)013<3560:ROTMJO>2.0.CO;2)
- Kiladis, G. N., Dias, J., Straub, K. H., Wheeler, M. C., Tulich, S. N., Kikuchi, K., Weickmann, K. M., & Ventrice, M. J. (2014). *A Comparison of OLR and Circulation-Based Indices for Tracking the MJO*. <https://doi.org/10.1175/MWR-D-13-00301.1>
- Kiladis, G. N., Wheeler, M. C., Haertel, P. T., Straub, K. H., & Roundy, P. E. (2009). *CONVECTIVELY COUPLED EQUATORIAL WAVES*.
- Kim, H., Janiga, M. A., & Pegion, K. (2019). MJO Propagation Processes and Mean Biases in the SubX and S2S Reforecasts. *Journal of Geophysical Research: Atmospheres*, *124*(16), 9314–

9331. <https://doi.org/10.1029/2019JD031139>

- Kim, H., Richter, J. H., & Martin, Z. (2019). Insignificant QBO-MJO Prediction Skill Relationship in the SubX and S2S Subseasonal Reforecasts. *Journal of Geophysical Research: Atmospheres*, 124(23), 12655–12666. <https://doi.org/10.1029/2019JD031416>
- Kim, Y.-H., Kiladis, G. N., Albers, J. R., Dias, J., Fujiwara, M., Anstey, J. A., Song, I.-S., Wright, C. J., Kawatani, Y., Lott, F., & Yoo, C. (2019). Comparison of equatorial wave activity in the tropical tropopause layer and stratosphere represented in reanalyses. *Atmospheric Chemistry and Physics Discussions*, 1–36. <https://doi.org/10.5194/acp-2019-110>
- Klotzbach, P., Abhik, S., Hendon, H. H., Bell, M., Lucas, C., G. Marshall, A., & Oliver, E. C. J. (2019). On the emerging relationship between the stratospheric Quasi-Biennial oscillation and the Madden-Julian oscillation. *Scientific Reports*, 9(1), 1–9. <https://doi.org/10.1038/s41598-019-40034-6>
- Lin, H., Brunet, G., & Derome, J. (2009). An observed connection between the North Atlantic oscillation and the Madden-Julian oscillation. *Journal of Climate*, 22(2), 364–380. <https://doi.org/10.1175/2008JCLI2515.1>
- Liu, C., Tian, B., Li, K.-F., Manney, G. L., Livesey, N. J., Yung, Y. L., & Waliser, D. E. (2014). Northern Hemisphere mid-winter vortex-displacement and vortex-split stratospheric sudden warmings: Influence of the Madden-Julian Oscillation and Quasi-Biennial Oscillation. *Journal of Geophysical Research: Oceans*, 8410–8421. <https://doi.org/10.1002/2014JC010261>.Received
- Madden, R. A., & Julian, P. R. (1971). Detection of a 40-50 Day Oscillation in the Zonal Wind in the Tropical Pacific. *Journal of the Atmospheric Sciences*.
- Madden, R. A., & Julian, P. R. (1972). Description of Global-Scale Circulation Cells in the Tropics with a 40-50 Day Period. *Journal of the Atmospheric Sciences*.
- Marshall, A. G., Hendon, H. H., Son, S. W., & Lim, Y. (2017). *Impact of the quasi-biennial oscillation on predictability of the Madden-Julian oscillation*. 49(4), 1365–1377. <https://doi.org/10.1007/s00382-016-3392-0>
- Mcintyre, E. (1982). How Well do we Understand the Dynamics of the Stratospheric Warmings? *Journal of the Meteorological Society of Japan, February*, 37–65.
- Naumann, G., & Vargas, W. M. (2010). Joint Diagnostic of the surface air temperature in southern South America and the Madden-Julian oscillation. *Weather and Forecasting*, 25(4), 1275–1280. <https://doi.org/10.1175/2010WAF2222418.1>
- Nishimoto, E., & Yoden, S. (2017). Influence of the stratospheric quasi-biennial oscillation on the Madden-Julian oscillation during austral summer. *Journal of the Atmospheric Sciences*, 74(4), 1105–1125. <https://doi.org/10.1175/JAS-D-16-0205.1>

- Roundy, P. E., Schreck, C. J., & Janiga, M. A. (2009). Contributions of convectively coupled equatorial Rossby waves and Kelvin waves to the real-time multivariate MJO indices. *Monthly Weather Review*, *137*(1), 469–478. <https://doi.org/10.1175/2008MWR2595.1>
- Scaife, A. A., Comer, R., Dunstone, N., Fereday, D., Folland, C., Good, E., Gordon, M., Hermanson, L., Ineson, S., Karpechko, A., Knight, J., MacLachlan, C., Maidens, A., Peterson, K. A., Smith, D., Slingo, J., & Walker, B. (2017). Predictability of European winter 2015/2016. *Atmospheric Science Letters*, *18*(2), 38–44. <https://doi.org/10.1002/asl.721>
- Straub, K. H. (2013). MJO initiation in the real-time multivariate MJO index. *Journal of Climate*, *26*(4), 1130–1151. <https://doi.org/10.1175/JCLI-D-12-00074.1>
- Taroh, B. (1966). *Quasi-Geostrophic Motions Equatorial Area* *. February, 25–43.
- Virts, K. S., & Wallace, J. M. (2014). Observations of temperature, wind, cirrus, and trace gases in the tropical tropopause transition layer during the MJO. *Journal of the Atmospheric Sciences*, *71*(3), 1143–1157. <https://doi.org/10.1175/JAS-D-13-0178.1>
- Wang, J., Kim, H. M., & Chang, E. K. M. (2018). Interannual Modulation of Northern Hemisphere Winter Storm Tracks by the QBO. *Geophysical Research Letters*, *45*(6), 2786–2794. <https://doi.org/10.1002/2017GL076929>
- Wang, S., Tippett, M. K., Sobel, A. H., Martin, Z. K., & Vitart, F. (2019). Impact of the QBO on Prediction and Predictability of the MJO Convection. *Journal of Geophysical Research: Atmospheres*, *124*(22), 11766–11782. <https://doi.org/10.1029/2019JD030575>
- Wheeler, M. C., & Hendon, H. H. (2004). An all-season real-time multivariate MJO index: Development of an index for monitoring and prediction. *Monthly Weather Review*, *132*(8), 1917–1932. [https://doi.org/10.1175/1520-0493\(2004\)132<1917:AARMMI>2.0.CO;2](https://doi.org/10.1175/1520-0493(2004)132<1917:AARMMI>2.0.CO;2)
- Wheeler, M., & Kiladis, G. N. (1999). Convectively Coupled Equatorial Waves: Analysis of Clouds and Temperature in the Wavenumber-Frequency Domain. *Journal of the Atmospheric Sciences*, *56*(3), 374–399. [https://doi.org/10.1175/1520-0469\(1999\)056<0374:CCEWAO>2.0.CO;2](https://doi.org/10.1175/1520-0469(1999)056<0374:CCEWAO>2.0.CO;2)
- Yoo, C., & Son, S. W. (2016). Modulation of the boreal wintertime Madden-Julian oscillation by the stratospheric quasi-biennial oscillation. *Geophysical Research Letters*, *43*(3), 1392–1398. <https://doi.org/10.1002/2016GL067762>
- Zhang, C., & Zhang, B. (2018). *QBO-MJO Connection*.